Title: Protein Quality Control is a Risk Factor and Therapeutic Target in Toxin-Induced Biliary Atresia

Short Title: Novel therapeutic target for biliary atresia

Authors: Xiao Zhao[1], Kristin Lorent[1], Diana Escobar-Zarate[1], Ramakrishnan Rajagopalan[2], Kathleen M. Loomes[3], Kevin Gillespie[4], Clementina Mesaros[4], Michelle A. Estrada[5], Ian Blair[4], Jeffrey D. Winkler[5], Nancy B. Spinner[3], Marcella Devoto[6,7,8], Michael Pack[1,9]*

Affiliations:

[1]Division of Gastroenterology, Department of Medicine, Perelman School of Medicine, University of Pennsylvania, Philadelphia, PA, USA.

[2]Division of Genomic Diagnostics, Department of Pathology, The Children's Hospital of Philadelphia and University of Pennsylvania Perelman School of Medicine, Philadelphia, PA, USA.

[3]Division of Gastroenterology, Hepatology and Nutrition, Department of Pediatrics, The Children's Hospital of Philadelphia and University of Pennsylvania Perelman School of Medicine, Philadelphia, PA, USA.

[4]Department of System Pharmacology and Translational Therapeutics, Perelman School of Medicine, University of Pennsylvania, Philadelphia, PA, USA.

[5]Department of Chemistry, University of Pennsylvania, Philadelphia, PA, USA.

[6]Division of Human Genetics, Children's Hospital of Philadelphia, Philadelphia, PA, USA.

[7]Departments of Pediatrics and of Biostatistics, Epidemiology and Informatics, Perelman School of Medicine, University of Pennsylvania, Philadelphia, PA, USA.

[8]Department of Translational and Precision Medicine, University La Sapienza, Rome, Italy.

[9]Department of Cell and Developmental Biology, Perelman School of Medicine, University of Pennsylvania, Philadelphia, PA 19104, USA.

Grant support:

This research was supported by NIH/NIDDK grants R01DK111547 to M.P., K08DK107910-01A1 and KL2TR001879 to X.Z., and R01 DK090045 to NS, MD, by the Fred and Suzanne Biesecker Pediatric Liver Center, NIH/NIEHS P30ES013508 and NIH/NCI P30CA016520 to IAB, and NIH/NIEHS T32ES019851 to KPG.

The Childhood Liver Disease Research Network is supported by U01 grants from the National Institute of Diabetes, Digestive and Kidney Disease (NIDDK): DK062481, DK062456, DK062497, DK084536, DK062500, DK062503, DK062466, DK062453, DK062452, DK062436, DK103149, DK103135, DK084575, DK084538, DK062470, DK103140 and DK062455. In addition, the project was supported by UL1 grants from the National Institutes of Health Clinical and Translational Sciences Award (CTSA) program through the National Center for Advancing Translational Science (NCATS): TR001872, TR001857, TR001108, TR002535, TR000454, TR000423, RR025014, TR000077 and TR000003.

Correspondence: mpack@pennmedicine.upenn.edu

Disclosures: None

Abbreviations: 17-AAG, 7-*N*-allylamino-17-demethoxygeldanamycin; BA, biliary atresia; bil, biliatresone; 8-Br-cGMP, 8-Bromoguanosine 3',5'-cyclic monophosphate; extrahepatic cholangiocytes; Gcl, glutamate cysteine ligase; GGA, geranylgeranyl acetate; gsr, *glutathione reductase*; GSH, reduced glutathione; GSSG, oxidized glutathione; IHC, intrahepatic cholangiocytes; HPE, hepatoportoenterostomy; NAC, *N*-acetylcysteine; *nuclear factor, erythroid*

2-like (*nrf2*); PDE5i, Phosphodiesterase-5 inhibitors; PQC, protein quality control; TLS (translesion DNA synthesis)

Abstract

BACKGROUND and AIMS: Extra-hepatic biliary atresia (BA) is an important pediatric liver disease with no approved medical therapy. Recent studies using human samples and experimental modeling suggest that glutathione redox metabolism and heterogeneity play an important role in disease pathogenesis. We sought to dissect the mechanistic basis of liver redox variation and to explore how other stress responses affect cholangiocyte injury in BA.

METHODS: We performed quantitative *in situ* hepatic glutathione redox mapping in zebrafish larvae carrying targeted mutations in glutathione metabolism genes and correlated these findings with sensitivity to the plant-derived BA-linked toxin biliatresone. We also determined whether genetic disruption of HSP90 protein quality control pathway genes implicated in human BA altered biliatresone toxicity in zebrafish and human cholangiocytes. An *in vivo* screen of a known drug library was performed to identify novel modifiers of cholangiocyte injury in the zebrafish experimental BA model with subsequent validation.

RESULTS: Glutathione metabolism gene mutations caused regionally distinct changes in the redox potential of cholangiocytes that differentially sensitized them to biliatresone. Disruption of human BA-implicated HSP90 pathway genes sensitized zebrafish and human cholangiocytes to biliatresone-induced injury independent of glutathione. Phosphodiesterase-5 inhibitors (PDE5i) and other activators of cGMP signaling worked synergistically with the glutathione precursor *N*-acetylcysteine (NAC) in preventing biliatresone-induced injury in zebrafish and human cholangiocytes. PDE5i functioned independently of glutathione but required intact HSP90 chaperone.

CONCLUSION: Regional variation in glutathione metabolism underlies sensitivity to the biliary toxin biliatresone, and mirrors recently reported BA risk stratification linked to

glutathione metabolism gene expression. Human BA can be causatively linked to genetic modulation of protein quality control. Combined treatment with NAC and PDE5i or other activators of cGMP signaling may block progression of BA.

Keywords: Chronic Liver Disease, cholestasis, glutathione metabolism

Extra-hepatic biliary atresia (BA) is a fibrosing cholangiopathy of infancy that is the most common indication for pediatric liver transplantation[1-4]. The etiology of BA has long been debated [4]. A minority of BA cases occurs as part of multi-organ developmental syndromes, thus supporting a genetic etiology; however, genetic factors have not been conclusively identified for the majority of cases, which occur in the absence of other defects (referred to as isolated BA). The most commonly accepted mechanistic model posits that BA is a complex disease resulting from exposure of genetically susceptible individuals to an environmental trigger, such as a toxin or virus, during late gestation[5-8]. In this model, exposure to commonly encountered agents would trigger BA in individuals with rare genetic variants, and conversely, rare exposures might trigger BA in individuals with common variants.

Using a zebrafish bioassay, we collaboratively isolated the electrophilic isoflavone biliatresone, from *Dysphania* species plants, whose maternal ingestion has been linked to epidemic BA in newborn livestock[9]. Biliatresone is the first environmental agent linked to a naturally occurring BA phenotype. Initial biochemical analyses suggested that the biliatresone alpha-methylene Michael acceptor, which is capable of forming adducts with reduced glutathione (GSH), nucleic acids and amino acids, was important for its toxicity[10, 11] . This was subsequently confirmed with structure activity relationship studies using zebrafish larvae and mammalian cholangiocyte spheroids [12]. Additional studies in the zebrafish model showed that the selective toxicity of biliatresone toward EHC correlated with intracellular glutathione redox potential, and that genetic disruption of *nuclear factor, erythroid 2-like* (*nrf2*), a key transcriptional regulator of anti-oxidant defenses [13], broadened biliatresone's toxicity profile, leading to destruction of the normally resistant intrahepatic cholangiocytes (IHC). These findings identified biliatresone as a

potent cellular oxidant. Supporting this injury model, treatment of zebrafish larvae and mouse cholangiocytes with the anti-oxidant N-acetylcysteine (NAC), a synthetic precursor of GSH, significantly delayed the onset of biliatresone toxicity[14, 15].

Although a causative role for an electrophilic toxicants in human BA is unproven, redox-mediated injury has been implicated in BA and two other human cholangiopathies, primary biliary cholangitis and primary sclerosing cholangitis[16-20]. The inciting injury in these conditions has not been determined, and likely differs from one another, however the disruption of defense mechanisms that allow cholangiocytes to withstand the oxidizing effect of continuous bile exposure is considered to be a common contributory factor. Hydrophobic bile acids in human bile have well characterized disruptive effects on mitochondrial function and proteostasis[21-25], and we speculate that stress-induced injury from bile acids can potentiate injury from environmental exposure to biliatresone or related agents.

Implicit in this model is the idea that genetic variants that modify cellular stress responses can be BA risk factors. Supporting this idea, hepatic expression of GSH metabolism genes at the time of Kasai portoenterostomy predicted transplant-free survival in infants with BA during the ensuing two years. This finding, coupled with the ability of NAC to reduce liver injury and fibrosis in the rotavirus murine BA model argue that progressive injury to mammalian IHC, which drives biliary fibrosis and ultimately liver failure in both conditions is influenced by cholangiocyte stress responses[26].

To gain a better understanding of the mechanisms underlying cholangiocyte sensitivity to redox

and proteomic stress, we examined how genetic manipulation of glutathione metabolism and heat shock chaperone-mediated protein quality control (PQC) affected biliatresone toxicity in zebrafish larvae and human cholangiocytes. Leveraging the screening capabilities of the zebrafish system, we identified pharmacological activators of cGMP signaling as protective of biliatresone-mediated injury, independent of glutathione metabolism but dependent on the Hsp70/Hsp90 chaperone system. Linking these findings to human BA, *de novo* genetic variants in the *STIP1* gene, which encodes the Hsp70-Hsp90 organizing protein (HOP), and *REV1*, which codes for a HSP90 client protein involved in replication stress[27,28], were recently identified in two children with isolated BA[29]. Collectively, the findings from this study suggest novel approaches to identify and treat children at risk for BA and other cholangiopathies.

Materials and Methods

Fish care and strains. The wild-type (WT) strains (TL, AB), transgenic strains (Tg (*ef1a*:Grx-roGFP; Tg(*Tp1*:mCherry), (*Tg(fabp10a:TRAP)*; (*Tg(krt18:TRAP)*) and mutant strains (*gclm*, *abcc2*, *gsr*, *stip1, rev1*) were used for the present studies. All zebrafish were raised in the University of Pennsylvania School of Medicine (Philadelphia, PA) zebrafish facility in accord with protocols approved by the University of Pennsylvania Institutional Animal Care and Use Committee.

Generation of targeted mutations in zebrafish using CRISPR/Cas9 system. The target sequences for *gclm, abcc2, stip1* were identified using the CHOPCHOP website: **Error! Hyperlink reference not valid.**. The single-guide RNA was generated as described[30]. Cas9 protein were obtained from PNABIO. Approximately 60 to 120 pg of sgRNA and 180 pg of Cas9 protein were co-injected into WT embryos at the one-cell stage. Genomic DNAs was

extracted from pools of 20 one-day old embryos, and the targeted areas were amplified and sequenced using primers listed in Supplementary Table 1 to confirm somatic mutations. Injected embryos were raised to adulthood (F0) and screened for the germline-transmitting founders. The F0 founders were subsequently outcrossed with WT fish to obtain the heterozygous F1 and F2 offspring. All experiments were performed on the animals of F3 or subsequent generations. The *gclm*, *abcc2* mutants were genotyped using primers listed in Table S1. The *gsr* and *stip1* mutant fish were genotyped using the KASP genotyping assays (KBioscience).

Redox-Sensitive GFP Redox Mapping Double transgenic (*Tg(ef1a:Grx-roGFP; tp1:mCherry*)) larvae in *gclm, abcc2, gsr* genetic background were used for the redox mapping of hepatocytes, IHCs, and EHCs. *Tg(ef1a:Grx-roGFP)* is a redox biosensor line previously generated in our laboratory. Conservation of the biosensor redox state was achieved with the thiol-alkylating agent, N-ethylmaleimide (NEM), and the protocol was adapted from a previous study of deep tissue fluorescence redox imaging in adult Drosophila and was performed as previously described [14, 31].

GSH Derivatization and Liquid Chromatography/Mass Spectrometry. The GSH content was measured in larvae livers of as previously described[14]. Five larval livers (including the extrahepatic biliary system) were used per sample.

Cell culture. H69 cells, an SV40-transformed (i.e. immortalized) normal human cholangiocyte cell line, and low passage number normal human cholangiocytes (NHCs) were obtained from Nicholas F. LaRusso (Mayo Clinic) and grown in H69 media as previously described [32].

Drug Treatments. Zebrafish larvae reared in 24-well plates were exposed to lyophilized biliatresone resuspended in anhydrous dimethyl sulfoxide (DMSO, 0.5% in embryo medium) for 24-72 hr. The larvae were either treated with low-dose biliatresone (0.25 μg/ml) or the standard dose (0.5 μg/ml) depending on the experimental condition. Additional compounds were used for the zebrafish studies at the indicated dose: N-acetylcysteine (NAC; Sigma-Aldrich; 20μM), aminophylline (Selleckchem, 100μM), vardenafil (Selleckchem, 1.5μM), tadalafil (Selleckchem, 1.5μM), 8-Bromoguanosine 3',5'-cyclic monophosphate (8-Br-cGMP, Sigma-Aldrich, 25μM), BAY 41-2272 (Sigma-Aldrich, 50μM), BAY 58-2667 (Sigma-Aldrich, 10μM), forskolin (Sigma-Aldrich, 0.5μM); 17-*N*-allylamino-17-demethoxygeldanamycin (17-AAG, Sigma-Aldrich, 13.2μM); geranylgeranyl acetate (GGA, Sigma-Aldrich, 20μM). The medium containing each compound was changed daily. All assays were repeated three times with at least 30 treated larvae and an equal number of control larvae in the zebrafish experiments.

Cultured cholangiocytes were serum starved for 24 hr prior to exposure to either low-dose biliatresone (0.50 μg/ml) or the standard dose (1.0 μg/ml) for 6-24 hr depending on the experimental condition. Additional compounds were used for the cell studies at the indicated dose: NAC (10μM), aminophylline (60μM), vardenafil (5μM), tadalafil (5μM), 8-Br-cGMP (500μM).

Immunofluorescence. After chemical treatments, larvae or cells were immunostaine with mouse monoclonal antibody Annexin A4 (Abcam, Cambridge, MA), or aceylated α-tubulin (Sigma-Aldrich), respectively, and processed for confocal microscopy as previously described [14]. Increased gain was applied to samples, if necessary, to visualize hypoplastic intrahepatic ducts in

zebrafish larval liver.

Nanostring nCounter assay and data analysis. Actively translating mRNA was extracted from larval hepatocytes and cholangiocytes (*Tg(fabp10a:TRAP)*; (*Tg(krt18:TRAP)*) using the translating ribosomal affinity purification (TRAP) methodology as previously described[14, 33]. *n* = 150-300 larvae dissected per condition. Gene expression analysis was performed with the nCounter system (NanoString Technologies) as previously described [14]. The input RNA was 100 ng per sample. The nCounter system uses molecular barcodes for direct digital detection of individual target mRNA molecules. The raw data were first normalized to the positive controls provided by the manufacturer, which accounted for variations in hybridization and purification efficiency, and then to three housekeeping genes (*bactin2*, *ef1a*, *rpl19*). The experiment was done in three biological replicates and differential gene expression was calculated relative to DMSO-treated controls.

siRNA Transfection. H69 cells were transfected with neg control siRNA (ON TARGET *plus* Non-targeting siRNA, Dharmacon), STIP1-iso1 siRNAs, STIP1-total siRNAs using DharmaFECT (Dharmacon) according to the manufacturer's protocol. Cells were subsequently treated with biliatresone (0.5 ug/ml) 48 hr post transfection for an additional 24 hr prior to further analyses. A 25 nM concentration of siRNA was used for all transfections.

RNA Extraction and qRT-PCR. RNA was isolated from zebrafish larval liver or cultured cholangiocytes using RNeasy Micro Kit (QIAGEN). RNA samples were quantified using a Nanodrop spectrophotometer (Thermo Fisher Scientific). Synthesis of cDNA from RNA samples

was carried out using the SuperScript III First-Strand Synthesis System (Thermo Fisher Scientific). Real-time RT PCR was performed using Applied Biosystems StepOnePlus and SYBR green PCR Master Mix (Thermo Fisher Scientific) with primers listed in Table S2.

Protein Extracts and Western Blots. Cells were lysed in Lysis M buffer (Roche), and lysates were sonicated and pelleted. Supernatants were denatured and 30ug of protein was separated by poly-acrylamide gel electrophoresis (Invitrogen), and then transferred to nitrocellulose membranes (Invitrogen). The following antibodies were used: STIP1 (Atlas Antibodies), REV1 (Santa Cruz, CA), β-actin (Santa Cruz, CA), and secondary anti-rabbit IgG (H+L)-HRP conjugate (Invitrogen) and anti-mouse IgG (H+L)-HRP conjugate (Invitrogen) antibodies. Enhanced chemiluminescence images were analyzed and quantified with ImageJ.

Cell Viability Assay. Cell viability assays were performed using tetrazolium compound based CellTiter 96® AQ_{ueous} One Solution Cell Proliferation (MTS) assay (Promega). Biliatresone-treated H69 were co-exposed to PDEI with and without NAC. MTS assay was then performed according to the manufacturer's instruction at 48 hr post-treatments.

Statistical Analyses. Data represent at least three independent experiments reported as means +/- SEM. The Student t test was used for comparison between two groups. Data from three or more groups were analyzed by one-way analysis of variance with Tukey's multiple comparisons test. $P < 0.05$ was considered to be significant.

Results

Genetic disruption of Glutathione metabolism genes in zebrafish

To gain insight into the differential sensitivity of zebrafish cholangiocytes to electrophilic stress, we analyzed the effect of biliatresone in larvae carrying loss-of-function mutations in glutathione metabolism genes. To study the role of glutathione synthesis and transport, we used CRISPR-Cas9 genome editing to disrupt *gclm*, which encodes the regulatory subunit of the rate-limiting enzyme in GSH synthesis, glutamate cysteine ligase (Gcl)[34], and *abcc2*[35], which encodes the canalicular transporter, Mrp2, that is required for GSH secretion from hepatocytes into bile. Mrp2 plays a central role in biliary GSH metabolism, as cholangiocytes synthesize GSH by degrading and resynthesizing GSH present in bile. Compared to the *gclm* mutation, which disrupts GSH synthesis in all cell types, mutation of *abcc2* specifically alters GSH synthesis in cholangiocytes. To study the role of GSH regeneration from its oxidized form GSSG[34], we analyzed larvae carrying a previously uncharacterized nonsense mutation in the *glutathione reductase* (*gsr*) gene (sa15125) that was generated *via* chemical mutagenesis (Fig. S1A, Table. S1).

Larvae homozygous for each mutation developed normally with normal hepatobiliary function and structure (Fig. S1B-D''). Adult mutants had normal fertility and lifespan with the locations of the nonsense mutations in all three genes (confirmed *via* genomic and cDNA sequencing) predicting either complete or significant loss of function (Fig. S1A). Supporting this, quantitative RT-PCR showed significantly reduced levels of each targeted transcript, presumably as a result of nonsense-mediated mRNA decay (Fig. S1E). Mass spectrometry studies also confirmed that each mutation had the predicted effect on GSH levels, namely a pronounced reduction in the total hepatic GSH content of *gclm* mutants compared to their WT siblings, as well as a

significant decrease in bile GSH measured in gallbladders dissected from adult *abcc2* mutants (Fig. S1F, G). Total hepatic GSH was not affected in *gsr* larvae, similar to *Gsr* mice[36] (Fig. S1F).

Mutations of glutathione metabolism genes alter cellular redox status

To determine how mutations in glutathione metabolism genes affect the basal glutathione redox state of different liver cell types, we crossed the mutant lines into transgenic fish carrying a ubiquitously expressed cytoplasmic redox biosensor Grx-roGFP2 (hereafter, roGFP) [14, 37]. This highly sensitive and specific *in vivo* probe contains an engineered dithiol/disulfide switch that provides a ratiometric readout of fluorescence emission at two excitation wavelengths (405 and 488 nm). A high 405nm:488nm excitation ratio indicates an oxidized sensor (low GSH:GSSG ratio), whereas a low ratio signifies a reduced state (high GSH:GSSG ratio).

Previous work showed that EHC of wild type zebrafish larvae are oxidized compared to IHC and hepatocytes, and that short duration exposure of larvae to biliatresone (4 hr) causes further oxidation of EHC, thus predicting overt injury that is first evident at 16-24 hr post-treatment[14]. Based on these earlier findings, we hypothesized that the effects of the glutathione metabolism gene mutations on basal glutathione redox status would provide insight into cellular sensitivities to oxidative stress, such as with exposure to biliatresone.

We first analyzed homozygous *gclm* mutants, whose dysfunctional GSH synthesis machinery, was predicted to oxidize the glutathione pool of EHC, IHC and hepatocytes. The roGFP measurements confirmed this prediction in the homozygotes, with normal hepatic redox heterogeneity observed in the wild type (WT) and heterozygous sibling larvae (Fig. 1A, B).

Next, we analyzed *gsr* mutants. Basal redox potential was also oxidized in all three liver cell types of homozygous mutants, most likely secondary to increased GSSG (Fig. 1C, D). However, oxidation was less than in *gclm* homozygotes, possibly reflecting a compensatory increase in GSH synthesis in Gsr deficient cells. Redox status was not altered in *gsr* heterozygotes (Fig. 1C, D). The *abcc2* mutation, which was predicted to have different effects on cholangiocytes and hepatocytes, was analyzed last. Homozygous *abcc2* mutation oxidized the glutathione pool of EHC and IHC, consistent with reduced GSH transport into bile, but had no effect on hepatocytes (Fig. S1G, 1E, F). Heterozygous mutation of *abcc2* oxidized the glutathione pool of EHC but not IHC, suggesting reduced GSH synthetic capacity in EHC compared to IHC (Fig. 1E, F).

Changes in redox status imparted by mutations in glutathione metabolism genes reveal cell-type specific responses to electrophilic stress

Having defined the effects of glutathione metabolism gene mutations on basal redox status, we next asked whether they were predictive of sensitization to biliatresone in either EHC or IHC. For this study, we define sensitization as EHC injury caused by a normally inactive low dose of the toxin (0.25 μg/ml; Fig. 2A, A', E), or IHC injury caused by either the low dose, or the standard dose (0.5 μg/ml), which only induces EHC injury in WT larvae (Fig. 2A, A'', E, F).

Previous studies of biliatresone in the zebrafish model suggested that oxidizing mutations would sensitize cholangiocytes to biliatresone [14]. Consistent with these predictions, we observed that the oxidized EHC of *gclm*, *abcc2* and *gsr* mutants were all sensitized to low dose biliatresone (Fig. 2B-C', D', E). The oxidized IHC of *gclm* homozygotes and *abcc2* homozygotes were sensitized to low and standard doses of the toxin, respectively (Fig. 2B, C''', F). Interestingly, basal redox

status was not always predictive of biliatresone sensitization. Specifically, we observed sensitization of IHC in *abcc2* heterozygotes and EHC in *gsr* heterozygotes, even though the basal redox potential was not significantly different from their WT siblings (Fig. 2C'', D, E, F). Conversely, the IHC of *gsr* homozygotes were resistant (not sensitized) to biliatresone despite their oxidation (Fig. 2D'', F).

Collectively, these findings identify important differences in the way EHC and IHC maintain redox homeostasis in response to oxidative stress. EHC, as evidenced by their sensitization in *gclm*, *abcc2*, and *gsr* mutants, rely on both GSH synthesis and GSH regeneration. In contrast, IHC rely only on GSH synthesis, as demonstrated by their resistance to biliatresone even when oxidized in regeneration-deficient *gsr* homozygotes. The importance of GSH synthesis in IHC is further underscored by their sensitization in non-oxidized *abcc2* heterozygotes.

Biliatresone induces proteomic stress and modulation of the Hsp90 chaperone machinery enhances biliatresone toxicity

Prior hepatic expression profiling experiments showed that in addition to glutathione metabolism genes, genes involved in the maintenance of cellular proteostasis were upregulated in the initial response to biliatresone [14]. Quantification of polysomal mRNA isolated from larval biliary cells (EHC & IHC) and hepatocytes *via* translating ribosomal affinity profiling (TRAP) methodology [33] confirmed the induction of heat shock response (HSR) and unfolded protein response/endoplasmic reticulum (UPR/ER) stress response genes in both cell types 4 hr after biliatresone exposure (Fig. 3A). To test the functional significance of these findings, we asked whether WT larvae treated with the heat shock protein 90 (Hsp90) inhibitor 17-*N*-allylamino-17-

demethoxygeldanamycin (17-AAG)[38, 39] were sensitized to low-dose biliatresone. Conversely, we also examined whether pre-treatment with geranylgeranyl acetate[40], an activator of heat shock protein 70 (Hsp70)[40, 41], which functions upstream of Hsp90 during the folding of newly synthesized and denatured proteins, could blunt biliatresone-mediated injury. We found that inhibition of Hsp90 sensitized EHC to low-dose biliatresone (Fig. 3B-C', E), whereas pre-treatment with the Hsp70 activator did not mitigate its toxic effect (Fig. 3D-E). Significantly, the GSH synthetic precursor NAC was unable to attenuate the sensitization caused by Hsp90 inhibition (Fig. 3C'', E). Altogether, these data suggest that the Hsp70/Hsp90 chaperone machinery plays a crucial role in the cellular response to biliatresone that is independent of the glutathione-mediated redox response.

Activation of cGMP signaling rescues biliatresone-mediated cholangiocyte injury in zebrafish and human cholangiocytes

The discovery that biliatresone affected protein quality control independently of redox homeostasis indicated that it might be possible to enhance the protective effect of NAC by activating other stress response pathways. To test this idea, we screened a library of known drugs (JHCC; Version 1.0) for their ability to blunt EHC damage in biliatresone-treated larvae. Of 1514 drugs screened, a consistent effect was only seen with two drugs, the phosphodiesterase inhibitors (PDEi) aminophylline and trequinsin. Aminophylline is a non-specific PDEi that blocks the hydrolysis of cAMP and cGMP in a broad range of cell types[42]. Trequinsin preferentially targets PDE isoform 3 (PDE3), also leading to increased levels of cAMP and cGMP[43, 44]. To confirm the specificity of these results, we co-treated larvae with standard dose biliatresone and independently sourced PDEi for 72 hr (Table S3). These experiments confirmed

the activity of aminophylline, with 56.0% of treated larvae exhibiting normal or minimally injured EHC (Fig. 4B, D), in contrast to 95% of larvae exhibiting severe EHC abnormalities that were treated biliatresone alone (Fig. 4A'). The response to trequinsin, on the other hand, was inconsistent (data not shown). Interestingly, two PDE5 inhibitors, vardenafil (Levitra) and tadalafil (Cialis), which block cGMP degradation and are clinically approved for erectile dysfunction and pulmonary hypertension[45, 46], had a comparable effect as aminophylline in 60.0% and 49.5% of the larvae examined, respectively (Fig. 4B', D, S2B, D).

To confirm that PDEi-mediated rescue arose from activation of cGMP signaling, we examined the effect of the cGMP analog 8-Bromoguanosine 3',5'-cyclic monophosphate (8-Br-cGMP)[36], and the heme-dependent and independent activators of soluble guanylate cyclase (sGC) (BAY 41-2272 and BAY 58-2667) in biliatresone-treated larvae. All three treatments imparted resistance to biliatresone that was comparable to treatments with the PDEi (Fig. 4B'', D; Fig. S2B', B'', D). In contrast, co-treatment with the adenylate cyclase activator, forskolin[39], which increases levels of cAMP, but not cGMP, did not reduce biliatresone-toxicity (Fig. S3)

Activation of cGMP signaling had a comparable effect on biliatresone toxicity in two human cholangiocyte cell lines (H69 and NHC)[47, 48]. On its own, standard dose biliatresone (1.0 μg/ml) disrupted microtubules, as evidenced by reduced immunostaining for α-tubulin, which was previously shown in biliatresone-treated mouse cholangiocytes[9, 15], and by decreased cell survival in both cell lines (Fig. 4E, E', H, S4A, A', D). Both toxicity readouts were significantly reduced by treatment with PDEi and 8-Br-cGMP (Fig. 4F-F'', H, S4B-B'', D). Interestingly, cGMP levels were not reduced by biliatresone (Fig. S5), suggesting that

endogenous cGMP signaling may not be affected by biliatresone. These findings confirm that activation of cGMP signaling can rescue biliatresone-mediated injury in both zebrafish and human cholangiocytes.

cGMP signaling functions independently of glutathione anti-oxidant responses

To examine the relationship of cGMP signaling to glutathione-mediated injury responses, we asked whether PDE5 inhibitors or 8-Br-cGMP enhanced the ability of NAC to delay EHC injury in biliatresone-treated zebrafish larvae. We found that activation of cGMP signaling in zebrafish significantly improved the effect of NAC, with 80-90% of larvae showing normal EHC or minimal EHC injury after 72 hr of treatment with standard dose biliatresone (Fig. 4C-D, S2C-D). NAC monotherapy, on the other hand, had no effect on biliatresone toxicity at this treatment time point (Fig. 4A'', D, S2A'', D). Highly comparable effects were also observed in co-treatment of the human cholangiocyte cell lines exposed to biliatresone (Fig. 4E'', G-H, S4A'', C-D).

As further proof that cGMP signaling functioned independently of glutathione-mediated responses, we examined the effect of vardenafil and 8-Br-cGMP in biliatresone-treated *gclm* mutants and observed significant mitigation of both EHC and IHD injury in the mutant larvae (Fig. S6A-E). Importantly, they did so without altering total hepatic GSH levels, which were reduced comparably in the mutants regardless of whether they received vardenafil or 8-Br-cGMP (Fig. S6F).

Validation of deleterious rare variants in the stress-induced HSP90 co-chaperone STIP1 and

HSP90 client protein REV1 in two children with BA

As part of an independent study, exome sequencing was performed in 30 probands with isolated BA ascertained through the NIDDK-funded Childhood Liver Disease Research Network[49] and their parents, to identify potentially causal *de novo* variants. Complete results of this large-scale exome sequencing project was recently reported elsewhere[29]. In one individual, a *de novo* heterozygous stop-gain variant (NP_001269581:p.(Cys30Ter)) was identified in the primate-specific isoform of the stress-inducible HSP90 co-chaperone *STIP1* (isoform 1)[29]. STIP1 is an evolutionarily conserved protein whose interactions with HSP70 and HSP90 orthologs have been demonstrated in yeast and rodents[50-52]. The BA-associated *STIP1* variant targets the longest transcript isoform, which possesses an additional 47 amino acids at the N- terminus compared to other protein isoforms. This variant was detected in the BA patient, but not present in either parent (familial relationships confirmed with exome data), and is found with a minor allele frequency of 0.002% (3 heterozygous alleles) in the population variant database gnomAD. In a second individual, a novel obligatory splice-site mutation was identified in the intron between exon 10 and exon 11 of the gene *REV1* that affects all isoforms. *REV1* encodes a Y-family polymerase that plays a central role in translesion DNA synthesis (TLS) during replication stress and has been shown to be a HSP90 client protein[27, 28,29].

To test the hypothesis that nonsense variant in *Stip1* or *Rev1* could exacerbate biliatresone-mediated injury, we first used CRISPR-Cas9 to engineer loss-of-function mutations in the zebrafish orthologs of these genes. The resulting frameshift mutations were confirmed *via* cDNA sequencing (Fig. S7A). Interestingly, whereas STIP1 knockout mice are embryonically lethal due to placental disruption, zebrafish deficient in Stip1 develop normally, but do not survive to

adulthood well. Of the 36 fish that survived to adulthood, there were 9 WT and 25 heterozygotes but only two mutants (2/36 = 5.6%). Although these mutant fish develop normally at 5 dpf, their ability to respond to toxic insults is compromised, including in heterozygous carriers. Specifically, we observed pronounced EHC injury in 75.0% heterozygous and 86.3% homozygous mutant larvae exposed to low-dose biliatresone (Fig. 5A-B'', D). Complementary observation of impaired stress tolerance was also made in the *rev1* mutant fish with 66.67% of heterozygotes and 90% of homozygotes showing severe EHC abnormality after low-dose toxin treatment (Fig. 5C-D).

To get a better understanding of the potential role of the *STIP1* isoform 1 mutation in human BA, we examined its expression in biliatresone-treated H69 cells. Interestingly, we found that while isoform-1 is not the predominant isoform in this cell type, its mRNA was up-regulated by 3.5 fold after 6 hr biliatresone exposure, whereas total *STIP1* mRNA was only increased 1.5 fold. To determine if isoform-1 affects cholangiocyte responses to biliatresone, we asked whether its selective knockdown, *via* siRNA, sensitized H69 cells to a low dose of the toxin by examining for evidences of impaired stress tolerance as well as decreased viability. RT-PCR showed significant reduction in *STIP1-iso1* mRNA levels (70.6%) with no significant effect on total *STIP1* mRNA levels (Fig. S7B). This specific knockdown caused a pronounced destabilization of microtubules in cells treated with low-dose biliatresone along with decreased cell survival, whereas no severe tubulin depolymerization or changes in cell viability was seen with the control siRNA (Fig. 5F-G', J). Similar sensitization to biliatresone was observed with siRNA that target all *STIP1* isoforms, which led to significant reduction in both isoform-1 mRNA (82.6%) and *STIP1* total mRNA (79.5%) (Fig. S7B, 5H, H', J). Western blot analyses showed that the non-

selective siRNAs significantly reduced STIP protein (49.9%) whereas the isoform-1 siRNAs had no effect, either because the antibody doesn't recognize isoform-1, or because the endogenous protein level of this isoform is low relative to the non-targeted isoforms (Fig. 5E).

Since STIP1 has been shown to promote DNA damage response (DDR)[53, 54], we also assessed for formation of nuclear foci of phosphorylated H2AX (γ-H2AX), which accumulate at sites of stalled replication forks and are a sensitive indicator of both DNA damage and replication stress. Interestingly, knockdown of total STIP1 protein led to induction of γ-H2AX foci in H69 cells treated with low-dose biliatresone, whereas no change in H2AX phosphorylation was observed with isoform-1 specific STIP1 knockdown (Fig. 5G-H'). Collectively, these data suggest that while STIP1 isoform-1 may play an important role in preventing cytoskeletal collapse mediated by exogenous electrophiles such as biliatresone, the other isoforms are essential for combatting oxidant-induced DNA damage.

Similar experiments were conducted in human cholangiocytes to examine the effect of REV1 depletion on biliatresone sensitivity. Treatment of H69 with REV1-specific siRNA resulted in significant REV1 knockdown, at both the mRNA and protein level (Fig. S7B, 5E). Although no apparent abnormality was observed in cells depleted of REV1 under unstressed conditions, pronounced accumulation of γ-H2AX associated with increased cell death was observed in cells exposed to low-dose biliatresone (Fig. 5I-J). Of note, REV1 knockdown did not lead to any apparent microtubule instability in cells treated with low-dose biliatresone, thus demonstrating a different injury mechanism than arises with STIP1 knockdown.

Mitigating effect of cGMP requires intact HSP70-HSP0- chaperone machinery in biliatresone-treated zebrafish and human cholangiocytes

cGMP signaling has been shown to enhance proteasome-mediated degradation of misfolded proteins in cardiomyocytes [55]. To determine whether cGMP functioned comparably in human cholangiocytes we first asked whether 8-Br-cGMP or PDE5i reversed upregulation of *HSP70* in biliatresone treated H69 cells. RT-PCR showed that this was the case, with near normalization of expression when both treatments were combined with NAC (Fig. 6A). To address this question with greater specificity in an *in vivo* setting, we asked if 8-Br-cGMP could ameliorate biliatresone toxicity in larvae with genetically or pharmacologically altered Hsp90/Hsp70 chaperone machinery. While we found that exogenous cGMP administration via 8-Br-cGMP could reverse sensitization of *stip1* homozygote mutants to biliatresone, the treatment failed to rescue biliatresone toxicity in zebrafish larvae co-exposed to the Hsp90 inhibitor 17-AAG, thus arguing that cGMP activity requires an intact Hsp90 in zebrafish. (Fig. 6B-D, F).

While functional Stip1 is not required for cGMP-mediated amelioration of cholangiocyte injury in zebrafish, modulation of this co-chaperone does impact the protective effect exerted by cGMP in biliatresone-treated human cholangiocytes. Specifically, we found that 8-Br-cGMP was able to mitigate biliatresone-induced disruption of α-tubulin in cells transfected with isoform-1 specific siRNAs, but not in cells with total STIP1 knockdown, arguing that cGMP in human cholangiocytes is sensitive to levels of STIP1 protein and/or a unique function of isoform-1 (Fig. 6G-I').

Although cGMP activity may be dependent on an intact HSP90/70 chaperone machinery, it does

not appear to rely on the HSP90 interacting protein REV1. Namely, we found that exogenous cGMP administration was able to attenuate EHD injury in *rev1* homozygous mutants and reverse γ-H2AX accumulation in biliatresone-treated REV1-depleted cells (Fig. 6E, F, J, J').

Short exposure to biliatresone leads to progressive EHD damage in zebrafish larvae, which can be halted by enhancing redox homeostasis and cGMP signaling

As an environmental trigger for human BA has not been conclusively demonstrated, the timing and duration of exposure remain speculative. The recent observation that a rising total bilirubin level had high sensitivity and specificity for BA in newborn infants [56] suggests a prenatal exposure, presumably transient, can trigger progressive and irreversible biliary damage. Supporting this model of biliary injury, we found that short exposure to standard dose biliatresone (6 hr) induced minimal or no EHC injury at the end of the exposure period, consistent with prior studies [14], however the injury progressed in 64.3% of larvae by 24 hr post-treatment despite toxin removal (Fig. 7A-B'', F). This suggests that once initiated, the damaging cascade amplifies and self perpetuates. We were able to halt this progression of injury by initiating combined treatment with the NAC & cGMP at the time of toxin removal, but not with NAC alone (Fig. 8C, F). We found that 78.9%-92.5% of larvae exposed to cGMP enhancers or the combination therapy exhibited normal EHC or minor epithelial damage compared with 35.7% of untreated larvae (Fig. 8B'', D-F).

Discussion

There is a significant need for new treatments for BA, which despite being a rare condition is the most common indication for liver transplantation in the pediatric population. Unfortunately,

neither the inciting disease trigger, which leads to fibrotic destruction of the extra-hepatic biliary system, nor the cause of progressive intra-hepatic bile duct disease and subsequent liver failure has been determined. A perinatal viral illness has been the leading hypothesis for many years, however no viral culprit has been conclusively implicated in the human disease[57, 58]. Recent findings argue that the developing extra-hepatic biliary system may be particularly susceptible to biliary injury as a result of factors affecting cholangiocyte maturation and or differentiation (REFS). Despite these advance, the cause of BA remains enigmatic.

The identification of biliatresone from *Dysphania* species plants was a significant advance for the field because it was the first conclusive evidence of a non-infectious environmental agent capable of causing BA[9]. And while direct consumption of biliatresone by humans is unlikely, the toxin-induced BA model has provided novel insights into cholangiocyte injury mechanisms, and through this, insights into genetic risk factors and new treatment strategies, complementing ideas that have emerged from other BA models, particularly the mouse rotavirus infection model [40, 59].

The work reported here builds on previous studies in zebrafish that identified cholangiocyte redox reserve as an important factor in the selective toxicity of biliatresone to EHC[14, 15]. Through *in vivo* measurement of redox potentials in glutathione metabolism gene mutants, we now show that EHC, with their low basal redox reserve, require both GSH regeneration and *de novo* GSH synthesis to combat oxidative stress. IHC, on the other hand, can tolerate a basal oxidized redox state associated with lack of GSH regeneration and remain poised to mitigate an exogenous oxidative insult. This most likely derives from their greater GSH synthetic capacity, as even a modest reduction as occurs in *abcc2* heterozygotes with normal basal redox status, sensitizes to

biliatresone. Sensitization of *abcc2* and *gsr* heterozygotes to biliatresone despite each mutant exhibiting normal basal redox potential highlights the possibility that redox gene variants could be otherwise silent risk factors for environmentally induced BA in humans.

The mechanism that accounts for differences in cholangiocyte GSH metabolism is unknown, however we hypothesize that it reflects the shared lineage of IHC and hepatocytes, which derive from a common progenitor[60]. Hepatocytes have an extraordinarily high synthetic capacity for GSH compared to other cell types[34], and this is likely to be epigenetically regulated, at least in part. From this, we speculate that in IHC, the chromatin landscape surrounding genes needed for GSH synthesis may provide an advantageous response to environmental and/or endogenous stressors. Notably, risk imparted by modulation of the epigenetic factors could be additive to genetic variants in GSH metabolism genes, which on their own impart a small heritable disease risk that is not easily detected by predictive algorithms of protein function. Supporting this model, in prior work we demonstrated DNA hypomethylation in IHC relative to hepatocytes in BA infants at either the time of diagnosis or surgical repair, but not in infants with other cholestatic liver diseases, or in non-liver disease controls[61].

The limited GSH synthetic capacity of EHC revealed by the genetic analyses reported here is consistent with previous work showing that the onset of biliatresone toxicity is delayed by treatment with the GSH precursor, NAC[14, 15]. Interestingly, NAC administration has recently been shown to reduce liver injury and biliary fibrosis and increased survival times in the rotavirus-BA mouse model. Furthermore, transplant-free survival of BA infants following Kasai portoenterostomy was also shown to be associated with elevated hepatic expression of GSH

metabolism genes[26]. Benefits afforded by NAC in the rotavirus model reflect reduced injury to IHC, which is consistent with increased susceptibility of zebrafish IHC to biliatresone when GSH synthesis is impaired (Fig. 2)[14]. In human BA, the effects of enhanced antioxidant capacity can impact clinical outcomes through multiple mechanisms, however it seems likely that reduced IHC injury and resulting biliary fibrosis play a contributory role. Collectively, these data suggest that redox metabolism may play a crucial role in driving BA pathogenesis regarding of the inciting event.

While NAC does provide protection against biliatresone, its effect is transient, likely because the toxin activates additional stress response pathways parallel to glutathione-mediated responses. Supporting this idea, transcriptional profiling showed pronounced activation of the heat shock chaperone system, which when disrupted pharmacologically, with the pan-Hsp90 inhibitor 17-AAG, or genetically, *via* mutating the co-chaperone *stip1* or HSP90 client protein *rev1*, sensitized the larvae to the toxin. The observed sensitization was not mitigated by NAC, arguing that the proteostasis pathways are activated by biliatresone independently of the initial glutathione-mediated redox response.

Altered proteostasis has not been previously implicated in human BA, however a proteomic study found that hepatic levels of the inducible HSP90 isoform HSP90AA were reduced 20-fold in newly diagnosed BA infants compared to neonates with other cholestatic liver diseases (*58*). Assigning causality of this association is complicated by the fact that BA is typically diagnoses at an advanced stage. Our findings that the heat shock pathway is activated by biliatresone in the zebrafish larvae, coupled with sensitization imparted by siRNA knockdown and mutation of

Stip1 and Rev1, which both interact with Hsp90, supports a causal role that the variants detected in these genes via exome sequencing are BA risk factors. The mechanism underlying this risk is uncertain. The *STIP1* variant is predicted to disrupt only the largest of the three translated transcripts. Although the precise function of this primate-specific isoform has not been determined, it was rapidly and significantly upregulated upon exposure to biliatresone and its selective knockdown was sensitizing, thus arguing that this isoform plays an essential role in the cholangiocyte stress response. Tubulin immunostainings indicate that STIP1 isoform-1 maintains cytoskeletal integrity under conditions of oxidative stress, while the other isoforms are needed for the DNA damage response, as evidenced by accumulation of γ-H2AX foci, which are indicative of stalled replication or DNA damage. Collectively, these results demonstrate that in addition to maintaining proteostasis, both HSP90 and STIP1 also play crucial roles in maintaining cytoskeletal integrity and genome stability. These are consistent with prior studies showing their interactions with tubulin[62-64] and in regulating diverse DDR pathways *via* facilitating the folding of multiple DNA repair proteins, including p53 [65] and those involved in TLS such as REV1[28].

Similar to our findings that *STIP1* and *REV1* haploinsufficiency lead to increased susceptibility to exogenous stressors such as biliatresone, mice and cells deficient in these genes also exhibit heightened sensitivity to certain stress-inducing conditions. For example, neurons of heterozygous *Stip1* knockout mice are highly sensitive to metabolic stress induced by cerebral ischemia [53], whereas cells deficient in Rev1 are defective in DDR as they are unable repair DNA interstrand crosslinks, which can be induced by chemical agents including electrophiles[66].

The BA-associated *STIP1* and *REV1* variants studied here have not previously been linked to human disease. Based on this, we argue that these rare heterozygous loss of function variants are normally well tolerated, however under conditions of environmental or endogenous stress, they can predispose carriers to BA. One of the challenges in studying the genetic underpinnings of complex diseases lies is assigning causality to variants of uncertain significance[67]. Our results point to the power of using experimental models to identify pathogenic pathways, which can then be modulated to interrogate candidate genes, hence functionally connecting genetic variations with disease-relevant phenotypes.

The potential therapeutic role for cGMP signaling activators in BA is a novel finding to emerge from this study. cGMP signaling has been studied extensively in the context of cardiovascular disease as a mediator of nitric oxide-induced smooth muscle relaxation (*36*). Our observations indicate that the mitigating effect provided by cGMP to biliatresone-induced injury is mediated, at least in part, by the PQC machinery, either by enhancing protein refolding *via* the HSP70/HSP90 chaperone machinery or promoting proteasome degradation of denatured protein [55]. cGMP activity depends on Hsp90 in the zebrafish larvae, however it does not appear to rely on the adapter protein Stip1 or the Hsp90 client protein Rev1. Specifically, cGMP did not impact biliatresone sensitization from Hsp90 inhibition but was able to confer protection in Stip1 and Rev1 knockout zebrafish. The role of STIP1 in mediating cGMP signaling appears more complicated in human cholangiocytes. cGMP prevented biliatresone-induced tubulin destabilization in H69 cells deficient in STIP1 isoform-1, but was unable to reverse the damage in cells with reduced levels of all STIP1 isoforms. The mechanism underlying this response is not known. cGMP level measurements argue that PDE5i and sGC stimulators do not simply

restore cGMP levels altered by the toxin, but more likely modulate compartmentalized cGMP signaling, which has been observed in other cell types[68, 69].

Based on the additive ameliorative effects of combined NAC/cGMP in the biliatresone model we propose that combined use of these FDA-approved drugs can be used to prevent BA progression. We envision two points of entry for the combination NAC/cGMP therapy in the timeline of BA. First, near the onset of extra-hepatic duct obstruction, which can be determined by measurement of conjugated bilirubin at birth and at 2-3 weeks of age, before the onset of symptoms[56]. This approach has a high sensitivity and specificity for detecting BA, and was recently validated in a larger multi-center study [70]. Given the severity and progressive nature of BA, and that both NAC and PDE5 inhibitors are well tolerated in infants[71-75], combining treatments at this time point may be the most effective strategy, particularly if confirmatory studies can be performed allowing for treatment discontinuation in non-responders and those found not to have BA. Going forward, substitution of PDE5i with activators or stimulators of cGMP might be considered.

The second point of entry for treatment of BA infants with NAC/cGMP would be at the usual time of diagnosis, at 1 to 2 months of age[56]. At this stage, there is irreversible damage to the extra-hepatic ductal system and varying degrees of portal fibrosis. Institution of NAC/cGMP therapy following the Kasai hepatoportoenterostomy (HPE), either on its own, or in combination with an immune modulator, has the potential to improve bile drainage post-HPE and reduce ongoing biliary injury that eventually culminates in biliary fibrosis. Administration of NAC/cGMP at this later stage has the benefit of preventing treatment of non-BA infants, albeit at the cost of treatment delay.

The cause of biliary fibrosis following restoration of bile flow post-HPE is unknown but presumably reflects persistent activation of cholangiocyte damage pathways triggered by the inciting injury, combined with bile acid-mediated injury and secondary activation of adaptive immunity. Given that temporary exposure of zebrafish larvae to biliatresone led to progressive injury, we speculate that activation of damage pathways following a transient environmental exposure can be self-sustaining, and that restoring redox and proteostatic homeostasis will be critical in preventing further biliary injury, thereby halting disease progression.

References

1. Haber BA, Russo P. Biliary atresia. Gastroenterol Clin North Am 2003;32:891-911.
2. Bezerra JA. Potential etiologies of biliary atresia. Pediatr Transplant 2005;9:646-51.
3. Schreiber RA, Barker CC, Roberts EA, et al. Biliary atresia: the Canadian experience. J Pediatr 2007;151:659-65, 665 e1.
4. Mack CL, Feldman AG, Sokol RJ. Clues to the etiology of bile duct injury in biliary atresia. Semin Liver Dis 2012;32:307-16.
5. Tsai EA, Grochowski CM, Loomes KM, et al. Replication of a GWAS signal in a Caucasian population implicates ADD3 in susceptibility to biliary atresia. Hum Genet 2014;133:235-43.
6. Garcia-Barcelo MM, Yeung MY, Miao XP, et al. Genome-wide association study identifies a susceptibility locus for biliary atresia on 10q24.2. Hum Mol Genet 2010;19:2917-25.
7. Cheng G, Tang CS, Wong EH, et al. Common genetic variants regulating ADD3 gene expression alter biliary atresia risk. J Hepatol 2013;59:1285-91.
8. Harper P, Plant JW, Unger DB. Congenital biliary atresia and jaundice in lambs and calves. Aust Vet J 1990;67:18-22.
9. Lorent K, Gong W, Koo KA, et al. Identification of a plant isoflavonoid that causes biliary atresia. Sci Transl Med 2015;7:286ra67.
10. Koo KW-Z, O; Wells, R; Pack, M; Porter J. Reactivity of Biliatresone, a Natural Biliary Toxin, with Glutathione, Histamine and Amino Acids. Chem Res Toxicol 2015;In Press
11. Koo KA, Lorent K, Gong W, et al. Biliatresone, a Reactive Natural Toxin from Dysphania glomulifera and D. littoralis: Discovery of the Toxic Moiety 1,2-Diaryl-2-Propenone. Chem Res Toxicol 2015;28:1519-21.
12. Estrada MA, Zhao X, Lorent K, et al. Synthesis and Structure-Activity Relationship Study of Biliatresone, a Plant Isoflavonoid That Causes Biliary Atresia. ACS Med Chem Lett 2018;9:61-64.

13. Hayes JD, Dinkova-Kostova AT. The Nrf2 regulatory network provides an interface between redox and intermediary metabolism. Trends Biochem Sci 2014;39:199-218.
14. Zhao X, Lorent K, Wilkins BJ, et al. Glutathione antioxidant pathway activity and reserve determine toxicity and specificity of the biliary toxin biliatresone in zebrafish. Hepatology 2016;64:894-907.
15. Waisbourd-Zinman O, Koh H, Tsai S, et al. Biliatresone, a toxin causing biliary atresia, causes cholangiocyte disruption and fibrosis and acts through a pathway involving decreased GSH and Sox17. Submitted 2015.
16. Grattagliano I, Calamita G, Cocco T, et al. Pathogenic role of oxidative and nitrosative stress in primary biliary cirrhosis. World J Gastroenterol 2014;20:5746-59.
17. Bell LN, Wulff J, Comerford M, et al. Serum metabolic signatures of primary biliary cirrhosis and primary sclerosing cholangitis. Liver Int 2015;35:263-74.
18. Petersen DR, Orlicky DJ, Roede JR, et al. Aberrant expression of redox regulatory proteins in patients with concomitant primary Sclerosing cholangitis/inflammatory bowel disease. Exp Mol Pathol 2018;105:32-36.
19. Wasik U, Milkiewicz M, Kempinska-Podhorodecka A, et al. Protection against oxidative stress mediated by the Nrf2/Keap1 axis is impaired in Primary Biliary Cholangitis. Sci Rep 2017;7:44769.
20. Leung PS, Choi J, Yang G, et al. A contemporary perspective on the molecular characteristics of mitochondrial autoantigens and diagnosis in primary biliary cholangitis. Expert Rev Mol Diagn 2016;16:697-705.
21. Yerushalmi B, Dahl R, Devereaux MW, et al. Bile acid-induced rat hepatocyte apoptosis is inhibited by antioxidants and blockers of the mitochondrial permeability transition. Hepatology 2001;33:616-26.
22. Sousa T, Castro RE, Pinto SN, et al. Deoxycholic acid modulates cell death signaling through changes in mitochondrial membrane properties. J Lipid Res 2015;56:2158-71.
23. Payne CM, Crowley-Skillicorn C, Holubec H, et al. Deoxycholate, an endogenous cytotoxin/genotoxin, induces the autophagic stress-survival pathway: implications for colon carcinogenesis. J Toxicol 2009;2009:785907.
24. Ferrebee CB, Li J, Haywood J, et al. Organic Solute Transporter alpha-beta Protects Ileal Enterocytes From Bile Acid-Induced Injury. Cell Mol Gastroenterol Hepatol 2018;5:499-522.
25. Li M, Cai SY, Boyer JL. Mechanisms of bile acid mediated inflammation in the liver. Mol Aspects Med 2017;56:45-53.
26. Luo Z, Shivakumar P, Mourya R, et al. Gene Expression Signatures Associated With Survival Times of Pediatric Patients With Biliary Atresia Identify Potential Therapeutic Agents. Gastroenterology 2019;157:1138-1152 e14.
27. Yoon JH, Park J, Conde J, et al. Rev1 promotes replication through UV lesions in conjunction with DNA polymerases eta, iota, and kappa but not DNA polymerase zeta. Genes Dev 2015;29:2588-602.
28. Pozo FM, Oda T, Sekimoto T, et al. Molecular chaperone Hsp90 regulates REV1-mediated mutagenesis. Mol Cell Biol 2011;31:3396-409.
29. Rajagopalan R, Tsai EA, Grochowski CM, et al. Exome sequencing in individuals with isolated biliary atresia. BioRxiv 831768. **[Preprint]**

30. Gagnon JA, Valen E, Thyme SB, et al. Efficient mutagenesis by Cas9 protein-mediated oligonucleotide insertion and large-scale assessment of single-guide RNAs. PLoS One 2014;9:e98186.
31. Seiler C, Davuluri G, Abrams J, et al. Smooth muscle tension induces invasive remodeling of the zebrafish intestine. PLoS Biol 2012;10:e1001386.
32. Tabibian JH, Trussoni CE, O'Hara SP, et al. Characterization of cultured cholangiocytes isolated from livers of patients with primary sclerosing cholangitis. Lab Invest 2014;94:1126-33.
33. Wilkins BJ, Gong W, Pack M. A novel keratin18 promoter that drives reporter gene expression in the intrahepatic and extrahepatic biliary system allows isolation of cell-type specific transcripts from zebrafish liver. Gene Expr Patterns 2014;14:62-8.
34. Lu SC. Glutathione synthesis. Biochim Biophys Acta 2013;1830:3143-53.
35. Jedlitschky G, Hoffmann U, Kroemer HK. Structure and function of the MRP2 (ABCC2) protein and its role in drug disposition. Expert Opin Drug Metab Toxicol 2006;2:351-66.
36. Yan J, Meng X, Wancket LM, et al. Glutathione reductase facilitates host defense by sustaining phagocytic oxidative burst and promoting the development of neutrophil extracellular traps. J Immunol 2012;188:2316-27.
37. Albrecht SC, Barata AG, Grosshans J, et al. In vivo mapping of hydrogen peroxide and oxidized glutathione reveals chemical and regional specificity of redox homeostasis. Cell Metab 2011;14:819-29.
38. Schulte TW, Neckers LM. The benzoquinone ansamycin 17-allylamino-17-demethoxygeldanamycin binds to HSP90 and shares important biologic activities with geldanamycin. Cancer Chemother Pharmacol 1998;42:273-9.
39. Yeyati PL, Bancewicz RM, Maule J, et al. Hsp90 selectively modulates phenotype in vertebrate development. PLoS Genet 2007;3:e43.
40. Bessho K, Mourya R, Shivakumar P, et al. Gene expression signature for biliary atresia and a role for interleukin-8 in pathogenesis of experimental disease. Hepatology 2014;60:211-23.
41. Ikeyama S, Kusumoto K, Miyake H, et al. A non-toxic heat shock protein 70 inducer, geranylgeranylacetone, suppresses apoptosis of cultured rat hepatocytes caused by hydrogen peroxide and ethanol. J Hepatol 2001;35:53-61.
42. Essayan DM. Cyclic nucleotide phosphodiesterases. J Allergy Clin Immunol 2001;108:671-80.
43. Jedlitschky G, Burchell B, Keppler D. The multidrug resistance protein 5 functions as an ATP-dependent export pump for cyclic nucleotides. J Biol Chem 2000;275:30069-74.
44. Friis UG, Jensen BL, Sethi S, et al. Control of renin secretion from rat juxtaglomerular cells by cAMP-specific phosphodiesterases. Circ Res 2002;90:996-1003.
45. Kukreja RC, Salloum FN, Das A. Cyclic guanosine monophosphate signaling and phosphodiesterase-5 inhibitors in cardioprotection. J Am Coll Cardiol 2012;59:1921-7.
46. Unegbu C, Noje C, Coulson JD, et al. Pulmonary Hypertension Therapy and a Systematic Review of Efficacy and Safety of PDE-5 Inhibitors. Pediatrics 2017;139.
47. Banales JM, Saez E, Uriz M, et al. Up-regulation of microRNA 506 leads to decreased Cl-/HCO3- anion exchanger 2 expression in biliary epithelium of patients with primary biliary cirrhosis. Hepatology 2012;56:687-97.

48. Grubman SA, Perrone RD, Lee DW, et al. Regulation of intracellular pH by immortalized human intrahepatic biliary epithelial cell lines. Am J Physiol 1994;266:G1060-70.
49. Thompson EJ, Perez K, Hornik CP, et al. Sildenafil Exposure in the Neonatal Intensive Care Unit. Am J Perinatol 2018.
50. Maciejewski A, Ostapchenko VG, Beraldo FH, et al. Domains of STIP1 responsible for regulating PrPC-dependent amyloid-beta oligomer toxicity. Biochem J 2016;473:2119-30.
51. Nicolet CM, Craig EA. Isolation and characterization of STI1, a stress-inducible gene from Saccharomyces cerevisiae. Mol Cell Biol 1989;9:3638-46.
52. Rohl A, Wengler D, Madl T, et al. Hsp90 regulates the dynamics of its cochaperone Sti1 and the transfer of Hsp70 between modules. Nat Commun 2015;6:6655.
53. Beraldo FH, Soares IN, Goncalves DF, et al. Stress-inducible phosphoprotein 1 has unique cochaperone activity during development and regulates cellular response to ischemia via the prion protein. FASEB J 2013;27:3594-607.
54. Karam JA, Parikh RY, Nayak D, et al. Co-chaperone Hsp70/Hsp90-organizing protein (Hop) is required for transposon silencing and Piwi-interacting RNA (piRNA) biogenesis. J Biol Chem 2017;292:6039-6046.
55. Ranek MJ, Terpstra EJ, Li J, et al. Protein kinase g positively regulates proteasome-mediated degradation of misfolded proteins. Circulation 2013;128:365-76.
56. Harpavat S, Garcia-Prats JA, Shneider BL. Newborn Bilirubin Screening for Biliary Atresia. N Engl J Med 2016;375:605-6.
57. Saito T, Shinozaki K, Matsunaga T, et al. Lack of evidence for reovirus infection in tissues from patients with biliary atresia and congenital dilatation of the bile duct. J Hepatol 2004;40:203-11.
58. Rauschenfels S, Krassmann M, Al-Masri AN, et al. Incidence of hepatotropic viruses in biliary atresia. Eur J Pediatr 2009;168:469-76.
59. Riepenhoff-Talty M, Schaekel K, Clark HF, et al. Group A rotaviruses produce extrahepatic biliary obstruction in orally inoculated newborn mice. Pediatr Res 1993;33:394-9.
60. Spence JR, Lange AW, Lin SC, et al. Sox17 regulates organ lineage segregation of ventral foregut progenitor cells. Dev Cell 2009;17:62-74.
61. Matthews RP, Eauclaire SF, Mugnier M, et al. DNA hypomethylation causes bile duct defects in zebrafish and is a distinguishing feature of infantile biliary atresia. Hepatology 2011;53:905-14.
62. Wu Y, Zheng X, Ding Y, et al. The molecular chaperone Hsp90alpha deficiency causes retinal degeneration by disrupting Golgi organization and vesicle transportation in photoreceptors. J Mol Cell Biol 2019.
63. Wu Y, Ding Y, Zheng X, et al. The molecular chaperone Hsp90 maintains Golgi organization and vesicular trafficking by regulating microtubule stability. J Mol Cell Biol 2019.
64. Li J, Sun X, Wang Z, et al. Regulation of vascular endothelial cell polarization and migration by Hsp70/Hsp90-organizing protein. PLoS One 2012;7:e36389.
65. Dahiya V, Agam G, Lawatscheck J, et al. Coordinated Conformational Processing of the Tumor Suppressor Protein p53 by the Hsp70 and Hsp90 Chaperone Machineries. Mol Cell 2019;74:816-830 e7.

66. Clauson C, Scharer OD, Niedernhofer L. Advances in understanding the complex mechanisms of DNA interstrand cross-link repair. Cold Spring Harb Perspect Biol 2013;5:a012732.
67. McAllister K, Mechanic LE, Amos C, et al. Current Challenges and New Opportunities for Gene-Environment Interaction Studies of Complex Diseases. Am J Epidemiol 2017;186:753-761.
68. Piggott LA, Hassell KA, Berkova Z, et al. Natriuretic peptides and nitric oxide stimulate cGMP synthesis in different cellular compartments. J Gen Physiol 2006;128:3-14.
69. Perera RK, Sprenger JU, Steinbrecher JH, et al. Microdomain switch of cGMP-regulated phosphodiesterases leads to ANP-induced augmentation of beta-adrenoceptor-stimulated contractility in early cardiac hypertrophy. Circ Res 2015;116:1304-11.
70. Harpavat S, Garcia-Prats JA, Anaya C, et al. Early detection and improved outcomes with large scale bilirubin screening for biliary atresia in more than 120,000 newborns. AASLD abstract 2019.
71. Perry HE, Shannon MW. Efficacy of oral versus intravenous N-acetylcysteine in acetaminophen overdose: results of an open-label, clinical trial. J Pediatr 1998;132:149-52.
72. Squires RH, Dhawan A, Alonso E, et al. Intravenous N-acetylcysteine in pediatric patients with nonacetaminophen acute liver failure: a placebo-controlled clinical trial. Hepatology 2013;57:1542-9.
73. Shiva A, Shiran M, Rafati M, et al. Oral Tadalafil in Children with Pulmonary Arterial Hypertension. Drug Res (Stuttg) 2016;66:7-10.
74. Sabri MR, Bigdelian H, Hosseinzadeh M, et al. Comparison of the therapeutic effects and side effects of tadalafil and sildenafil after surgery in young infants with pulmonary arterial hypertension due to systemic-to-pulmonary shunts. Cardiol Young 2017;27:1686-1693.
75. Tan K, Krishnamurthy MB, O'Heney JL, et al. Sildenafil therapy in bronchopulmonary dysplasia-associated pulmonary hypertension: a retrospective study of efficacy and safety. Eur J Pediatr 2015;174:1109-15.

Figure Legends

Fig. 1. Genetic disruption of glutathione metabolism genes in zebrafish differentially alter EHC, IHC and hepatocyte basal redox status. (A, C, E) *In situ* measurement of basal glutathione redox potential. Representative composite confocal images through the livers of gclm (A), gsr (C), abcc2 (E) bigenic mutant larvae Tg (*e1f*: Grx1-roGFP; *tp1:*mCherry). Glutathione redox status of EHC (gallbladder-dashed red circle), IHC, and

hepatocytes was derived from the roGFP 405nm/488nm fluorescence excitation ratio. Color bar on right (a higher excitation ratio indicates a more oxidized environment). EHC and hepatocytes localized by morphology. IHC localized by mCherry expression (pseudo-colored green to show location relative to hepatocytes). White dashed line - liver border. Scale bar, 10 µm. (B, D, F) Mean fluorescent 405 nm/488 nm excitation ratios in EHC, IHC, and hepatocytes for each genotype. n =10 larvae per genotype, means +/- SEM, *$p<0.02$ in comparison to WT EHC, IHC, or hepatocytes, respectively, per ANOVA with Tukey's multiple comparison test. EHC, extrahepatic cholangiocytes; IHC, intrahepatic cholangiocytes; H, hepatocytes.

Fig. 2. Glutathione metabolism gene mutations differentially sensitize cholangiocytes to biliatresone. Confocal projections through the livers of 6 dpf WT (A-A''), *gclm* (B), *abcc2* (C-C'''), *gsr* (D-D'') mutant larvae exposed to low-dose or standard dose biliatresone for 24 hr. All larvae immunostained with anti-Annexin A4 antibody. White arrow – Gallbladder; red arrow – gallbladder remnant. * denotes liver with IHC injury. Scale bar, 20 µm. (E) Percentage of *gclm, abcc2*, *gsr* mutant larvae and their WT sibling controls with severe EHC abnormalities after low-dose biliatresone exposure. (F) Percentage of *gclm, abcc2* mutant larvae and their WT siblings with IHC abnormalities after biliatresone exposure (either low-dose or standard dose). *n* = 30-36

per genotype per condition, means +/- SEM, *p<0.001 in comparison to WT control EHC or IHC, per ANOVA with Tukey's multiple comparison test. bil low, low-dose biliatresone; bil std, standard dose biliatresone; EHC, extrahepatic cholangiocytes, IHC, intrahepatic cholangiocytes; WT, wildtype.

Fig. 3. Hsp90 inhibition sensitizes EHC to biliatresone. (A) Expression of heat shock response and unfolded protein response genes in biliatresone-treated larval hepatocytes and cholangiocytes *versus* DMSO-treated controls as determined by nCounter technology. means +/- SEM, *p<0.02 in comparison to DMSO-treated control larvae by two-tailed unpaired student *t* test. (B-D) Confocal projections through the livers of 6 dpf larvae immunostained with anti-Annexin A4 antibody. (B-B'') WT control larva, and sibling larvae exposed to either low-dose, or standard dose biliatresone. (C-C'') 6 dpf larvae exposed to 17-AAG alone, 17-AAG with low-dose biliatresone, or 17-AAG with low-dose biliatresone and NAC. (D-D') 6 dpf larvae exposed to GGA or GGA and standard dose biliatresone. All exposures for 24 hr. White arrow – Gallbladder; red arrow – gallbladder remnant. Scale bar, 20 μm. (E) Percentage of larvae exposed to biliatresone, biliatresone & 17-AAG, or biliatresone & GGA with severe EHC abnormalities. *n* = 30-32 per condition, mean +/- SEM, *p<0.001 in comparison to control larvae per ANOVA with Tukey's multiple comparison test. bil low, low-dose biliatresone; bil std, standard dose biliatresone; EHC, extrahepatic cholangiocytes, 17-AAG, 17-*N*-allylamino-17-demethoxygeldanamycin; GGA, geranylgeranyl acetate; NAC, N-acetylcysteine.

Fig. 4. Activation of cGMP signaling attenuates biliatresone-mediated biliary injury in the zebrafish and human cholangiocytes. Confocal projections through the livers of 8 dpf larvae

immunostained with anti-Annexin A4 antibody. (A-A'') WT control larva, and WT larvae treated with standard dose biliatresone, or biliatresone and NAC. (B-B'') Larvae treated with biliatresone and PDE inhibitors (aminophylline or vardenafil), or biliatresone and 8-Br-cGMP. (C-C'') Larvae treated with biliatresone, PDE inhibitors and NAC, or biliatresone, 8-Br-cGMP and NAC. All exposures for 72 hr. White arrow – Gallbladder; red arrow – gallbladder remnant. Scale bar, 20 μm. (D) Percentage of biliatresone-treated larvae exposed to the indicated cGMP modulators with normal or minimally injured EHC. *n* = 30-36 per condition, mean +/- SEM, *p<0.001 in comparison to biliatresone-treated larvae per ANOVA with Tukey's multiple comparison test. (E-) H69 cells immunostained with anti-acetylated tubulin antibody (green) with DAPI (blue) counterstain. (E) Control cells; (E'-E'') cells treated with standard dose biliatresone with and without NAC. (F-F'') Cells treated with biliatresone and cGMP modulators (aminophylline, vardenafil, 8-Br-cGMP). (G-G'') Cells treated with biliatresone, cGMP modulators and NAC. Scale bar, 10 μm. (H) Viability of biliatresone-treated H69 cells co-exposed to cGMP modulators with and without NAC as determined by MTS assay. Results are expressed as a percentage of control (DMSO-treated cells) ± SEM, *p<0.001 in comparison to biliatresone-treated H69 cells per ANOVA with Tukey's multiple comparison test.bil, biliatresone; EHC, extrahepatic cholangiocytes; 8-Br-cGMP, 8-Bromoguanosine 3',5'-cyclic monophosphate; NAC, N-acetylcysteine.

Fig. 5. Stip1 and Rev1 disruption sensitizes zebrafish and human cholangiocytes to biliatresone. (A-C'') Confocal projections through the livers of 6 dpf larvae immunostained with anti-Annexin A4 antibody: wt larvae (A-A') and *stip1* (B-B''), *rev1* (C-C'') larvae treated with DMSO *versus* low-dose biliatresone for 24 hr. White arrow – Gallbladder; red arrow –

gallbladder remnant. (D) Percentage of wt, *stip1* and *rev1* larvae with severe EHC abnormalities after exposure to low-dose biliatresone. *n* = 30 per genotype and condition, mean +/- SEM, *p<0.001 in comparison to control larvae per ANOVA with Tukey's multiple comparison test. (E) Western blot showing protein levels of STIP1 and REV1 extracted from H69 cells 48 hr post transfection with negative control siRNA, STIP1-isoform 1 siRNA, STIP1-total siRNA, REV1 siRNA. (F-I') H69 cells immunostained with anti-acetylated tubulin antibody (green), anti-γH2AX (red) and DAPI (blue) counter stain. Cells treated with negative control siRNA (F) or negative control siRNA followed by low-dose biliatresone (F'). Cells transfected with STIP1-isoform 1 siRNA (G), STIP1-total siRNA (H) REV1 siRNA (I) followed by low-dose biliatresone (G', H', I'). Scale bar, 10 μm. (J) Bar graphs of relative cell viability of H69 cells transfected with control siRNA, STIP1-iso1 siRNA, STIP1-total siRNA, or REV1-siRNA followed by exposure to low-dose biliatresone as determined by MTT assay. Results are expressed as a percentage of control ± SEM, *p<0.001 in comparison to H69 cells treated with control siRNA per ANOVA with Tukey's multiple comparison test. bil low, low-dose biliatresone; EHC, extrahepatic cholangiocytes; STIP1-iso1, STIP1 isoform 1.

Fig. 6. cGMP rescue of biliatresone toxicity is dependent on heat shock proteostasis. (A) Relative HSP70 expression in H69 cells 24 hr post-treatment with DMSO (control), biliatresone, biliatresone and NAC, biliatresone and PDE inhibitors (aminophylline, vardenafil) on their own or combined with NAC. n = 3 replicates per condition, mean +/- SEM, *p<0.001 in comparison to control cells per ANOVA with Tukey's multiple comparison test. (B-E) Confocal projections through livers of biliatresone-treated WT, *stip1*, or *rev1* larvae immunostained with Annexin-A4 antibody comparing the effect of 8-Br-cGMP. White arrow – Gallbladder; red arrow –

gallbladder remnant. Scale bar, 20 μm. (F) Bar graph showing the percentage of WT, *stip1*, or *rev1* larvae larvae treated with biliatresone with normal or minimally injured EHC following co-treatment with 8-Br-cGMP. n = 30 per genotype per condition, mean +/- SEM, *p<0.001 in comparison to larvae treated with standard-dose biliatresone per ANOVA with Tukey's multiple comparison test. (G-J') H69 cells immunostained with anti-acetylated tubulin antibody (green), anti-γH2AX (red) and DAPI (blue) counterstain. Cells treated with negative control siRNA (G) or negative control siRNA followed by biliatresone with or without 8-Br-cGMP (G'-G'''). Cells transfected with STIP1-isoform 1 siRNA (H, H'), STIP1-total siRNA (I, I'), or REV1 siRNA (J, J') followed by low-dose biliatresone with or without 8-Br-cGMP. Scale bar, 10 μm. bil low, low-dose biliatresone; bil std, standard dose biliatresone; EHC, extrahepatic cholangiocytes, 17-AAG, 17-N-allylamino-17-demethoxygeldanamycin; 8-Br-cGMP, 8-Bromoguanosine 3',5'-cyclic monophosphate, STIP1-iso1, STIP1 isoform 1.

Fig. 7 Short term biliatresone exposure triggers EHC injury that is blocked by cGMP. (A) Experimental scheme depicting treatment of zebrafish larvae with standard dose biliatresone for 6 hr, followed by incubation with cGMP modulators (vardenafil or 8-Br-cGMP) with and without NAC for 24 hr. (B-E) Confocal projections through the livers of 5-6 dpf larvae immunstained with anti-Annexin A4 antibody. (B) Control larva, (B'-B'') Larvae exposed to biliatresone alone imaged 6 hr and 24 hr post treatment initiation, respectively. (C-E) Larvae treated with biliatresone for 6 hr followed by treatment with NAC (C); vardenafil +/- NAC (D-D'); 8-Br-cGMP +/- NAC (E-E') for 24 hr. Scale bar, 20 μm. (F) Percentage of larvae exhibiting normal or minimally injured EHC after biliatresone exposure for 6 hr followed by treatments with NAC/cGMP modulators. *n* = 30-35 per condition, mean +/- SEM, *p<0.001 in comparison

to control larvae per ANOVA with Tukey's multiple comparison test. bil, biliatresone; EHC, extrahepatic cholangiocytes; 8-Br-cGMP, 8-Bromoguanosine 3',5'-cyclic monophosphate; NAC, N-acetylcysteine.

Fig. 1

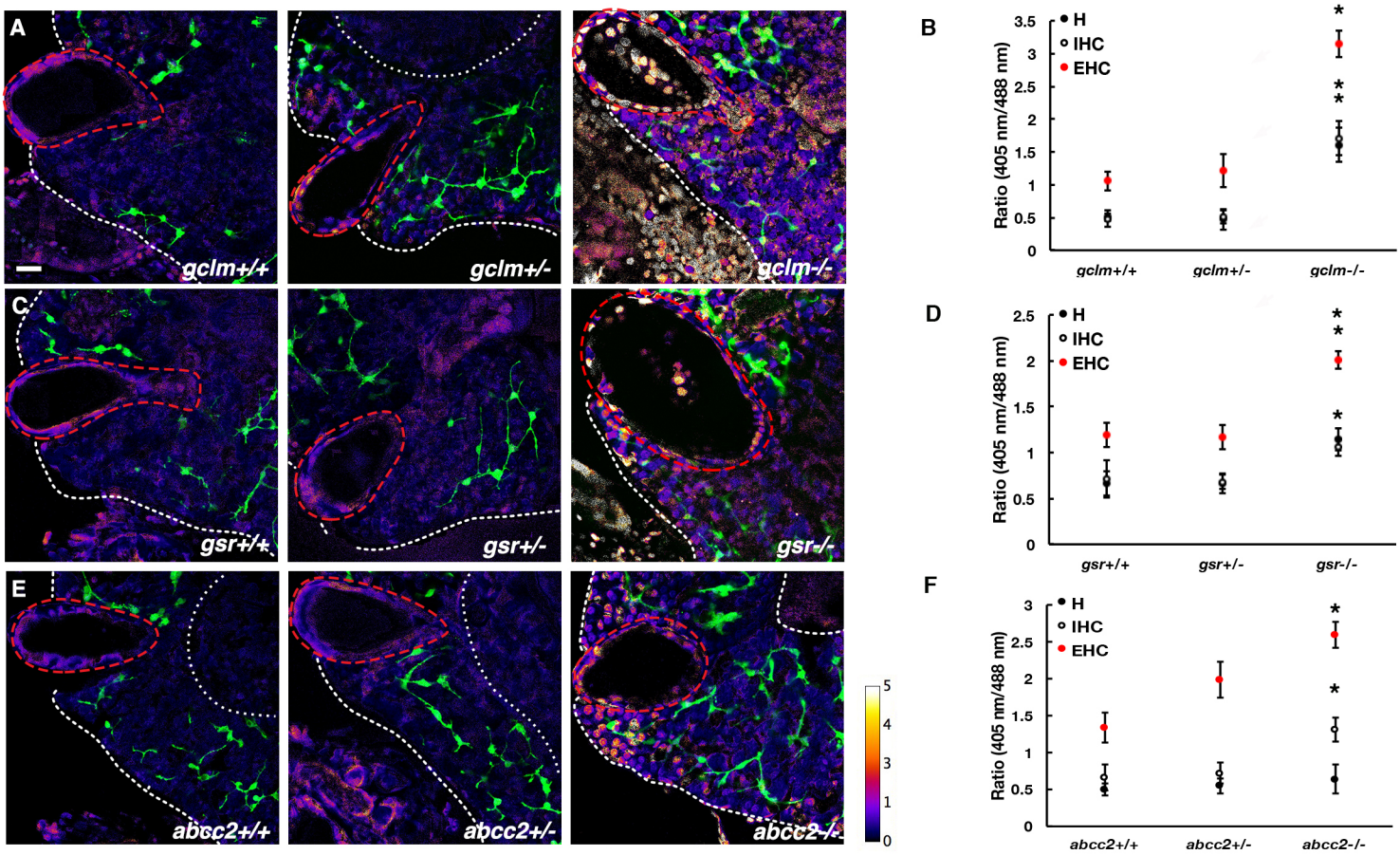
A
gclm+/+
gclm+/-
gclm-/-
C
gsr+/+
gsr+/-
gsr-/-
E
abcc2+/+
abcc2+/-
abcc2-/-
5
4
3
1
0
B
H
IHC
EHC
Ratio (405 nm/488 nm)
3.5
3
2.5
2
1.5
1
0.5
0
gclm+/+
gclm+/-
gclm-/-
D
H
IHC
EHC
Ratio (405 nm/488 nm)
2.5
2
1.5
1
0.5
0
gsr+/+
gsr+/-
gsr-/-
F
H
IHC
EHC
Ratio (405 nm/488 nm)
3
2.5
2
1.5
1
0.5
0
abcc2+/+
abcc2+/-
abcc2-/-

Fig. 2

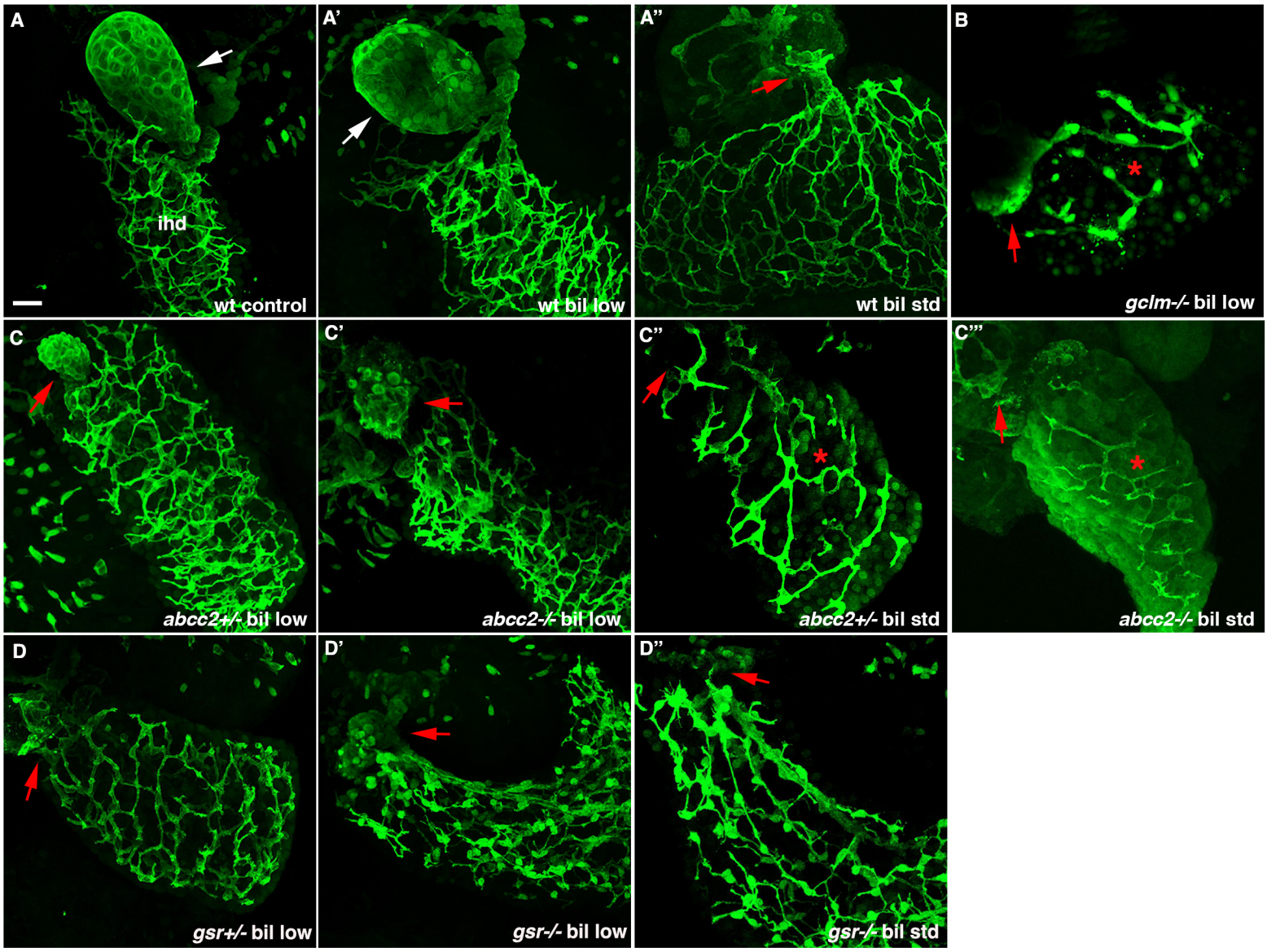
A
ihd
wt control
A'
wt bil low
A"
wt bil std
B
gclm-/- bil low
C
abcc2+/- bil low
C'
abcc2-/- bil low
C"
abcc2+/- bil std
C'''
abcc2-/- bil std
D
gsr+/- bil low
D'
gsr-/- bil low
D"
gsr-/- bil std

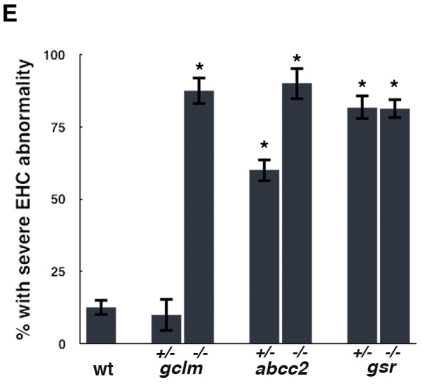
E
% with severe EHC abnormality
100
75
50
25
0
wt
+/-
-/-
gclm
abcc2
gsr

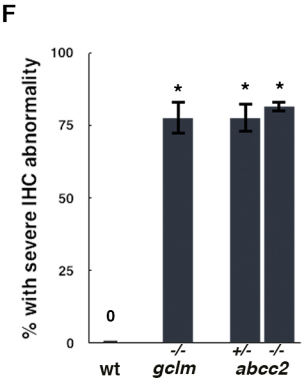
F
% with severe IHC abnormality
100
75
50
25
0
0
wt
-/-
gclm
+/-
abcc2

Fig. 3

A

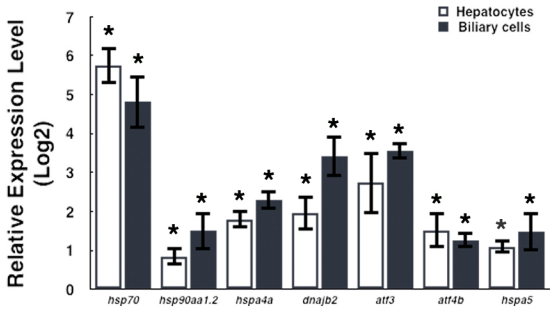
Hepatocytes
Biliary cells
Relative Expression Level (Log2)
0
1
2
3
4
5
6
7
hsp70
hsp90aa1.2
hspa4a
dnajb2
atf3
atf4b
hspa5

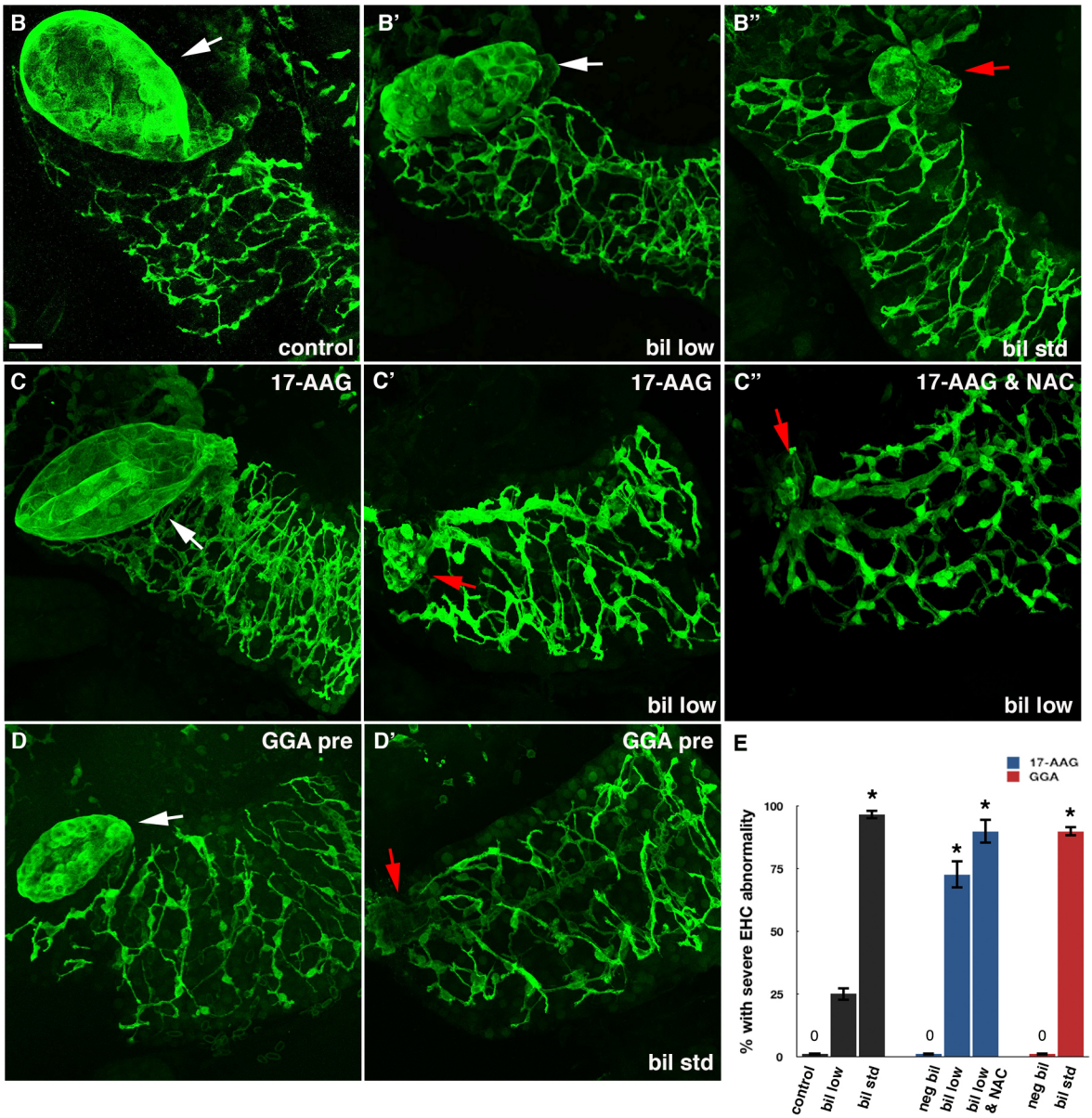
B
control
B'
bil low
B''
bil std
C
17-AAG
C'
17-AAG
bil low
C''
17-AAG & NAC
bil low
D
GGA pre
D'
GGA pre
bil std
E
17-AAG
GGA
% with severe EHC abnormality
0
25
50
75
100
control
bil low
bil std
neg bil
bil low
bil low & NAC
neg bil
bil std

Fig. 4

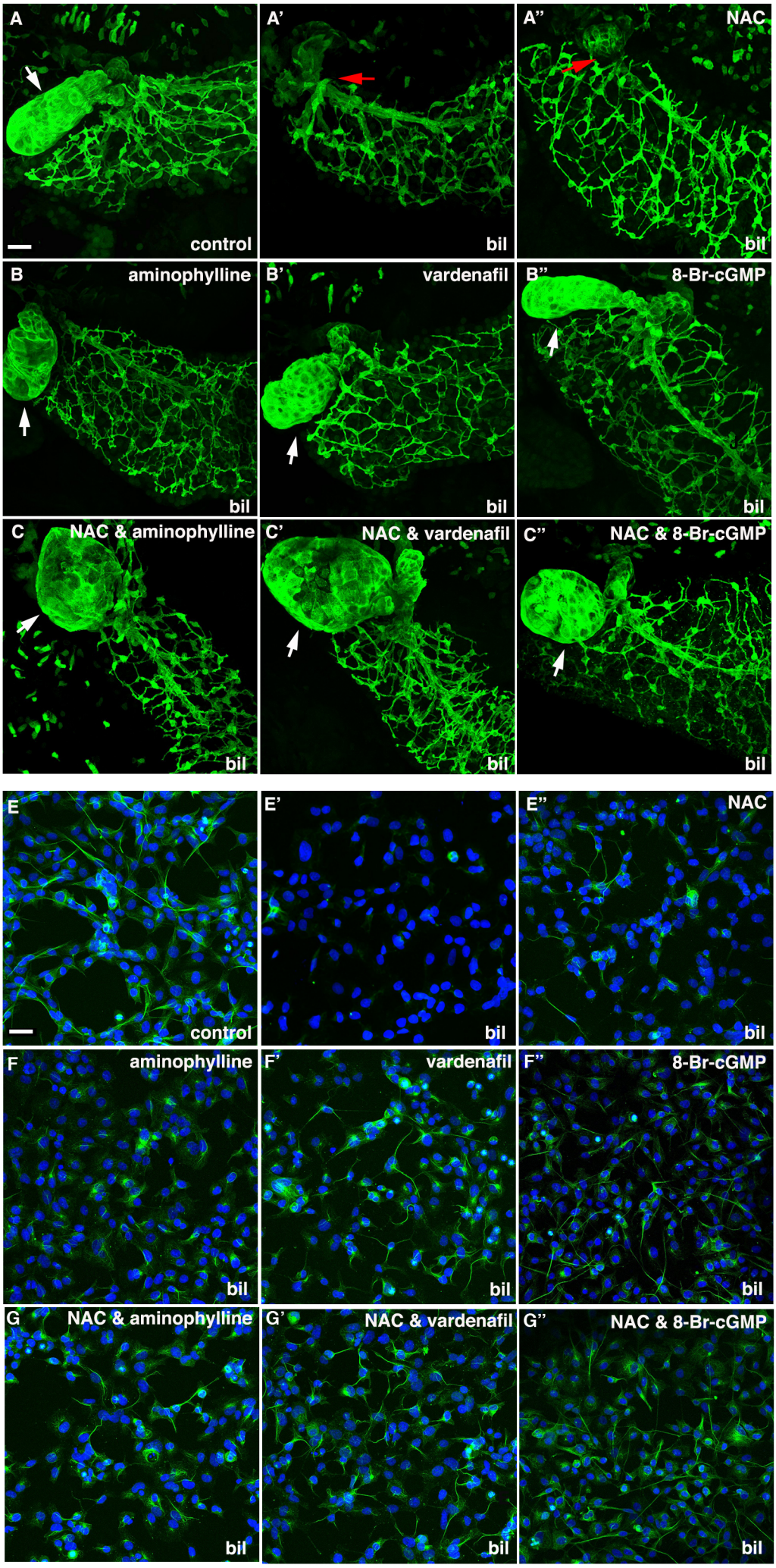
A
control
A'
bil
A''
NAC
bil
B
aminophylline
bil
B'
vardenafil
bil
B''
8-Br-cGMP
bil
C
NAC & aminophylline
bil
C'
NAC & vardenafil
bil
C''
NAC & 8-Br-cGMP
bil
E
control
E'
bil
E''
NAC
bil
F
aminophylline
bil
F'
vardenafil
bil
F''
8-Br-cGMP
bil
G
NAC & aminophylline
bil
G'
NAC & vardenafil
bil
G''
NAC & 8-Br-cGMP
bil

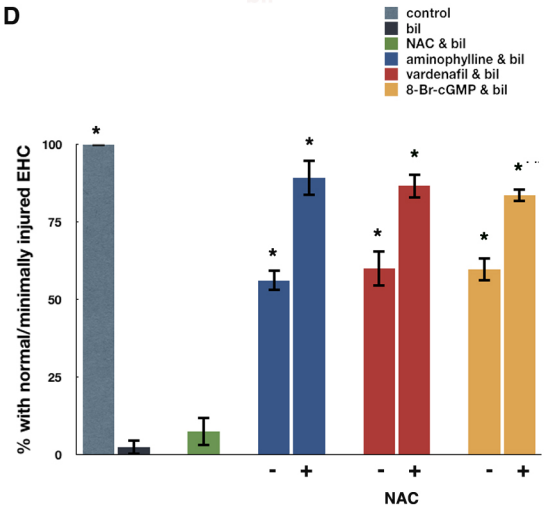
D
control
bil
NAC & bil
aminophylline & bil
vardenafil & bil
8-Br-cGMP & bil
% with normal/minimally injured EHC
100
75
50
25
0
-
+
-
+
-
+
NAC

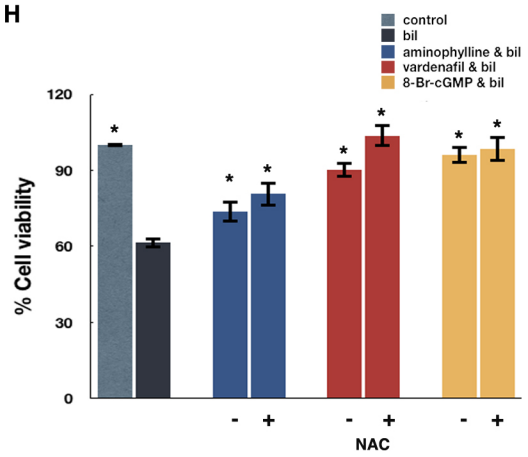
H
control
bil
aminophylline & bil
vardenafil & bil
8-Br-cGMP & bil
% Cell viability
120
90
60
30
0
-
+
-
+
-
+
NAC

Fig. 5

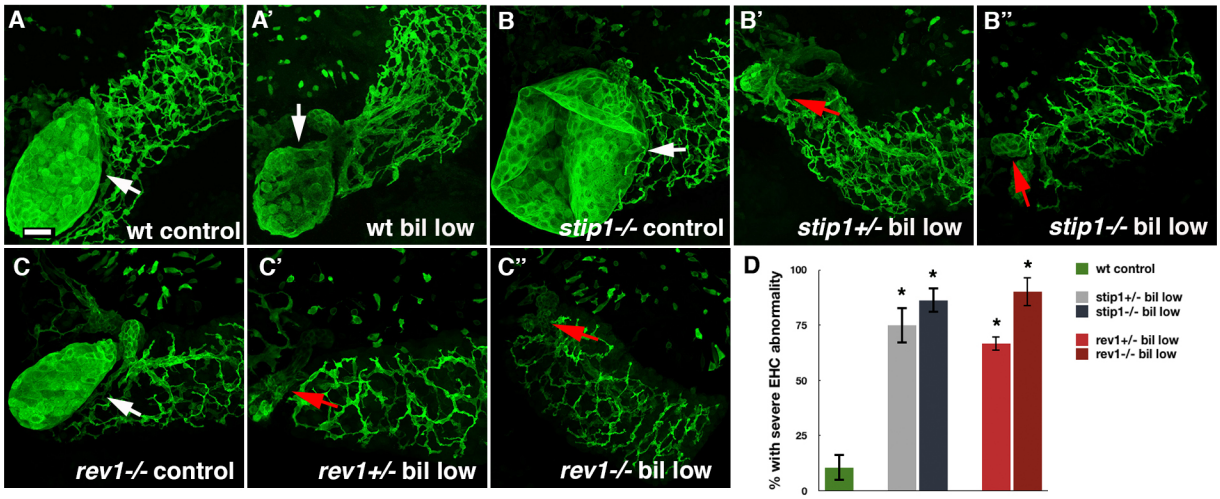
A
wt control
A'
wt bil low
B
stip1-/- control
B'
stip1+/- bil low
B''
stip1-/- bil low
C
rev1-/- control
C'
rev1+/- bil low
C''
rev1-/- bil low
D
% with severe EHC abnormality
100
75
50
25
0
wt control
stip1+/- bil low
stip1-/- bil low
rev1+/- bil low
rev1-/- bil low

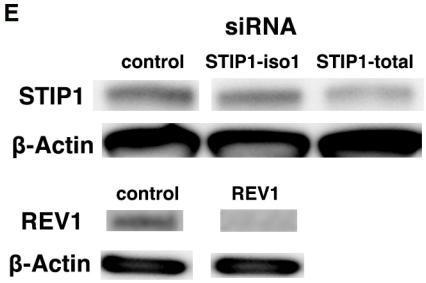
E
siRNA
control
STIP1-iso1
STIP1-total
STIP1
β-Actin
control
REV1
REV1
β-Actin

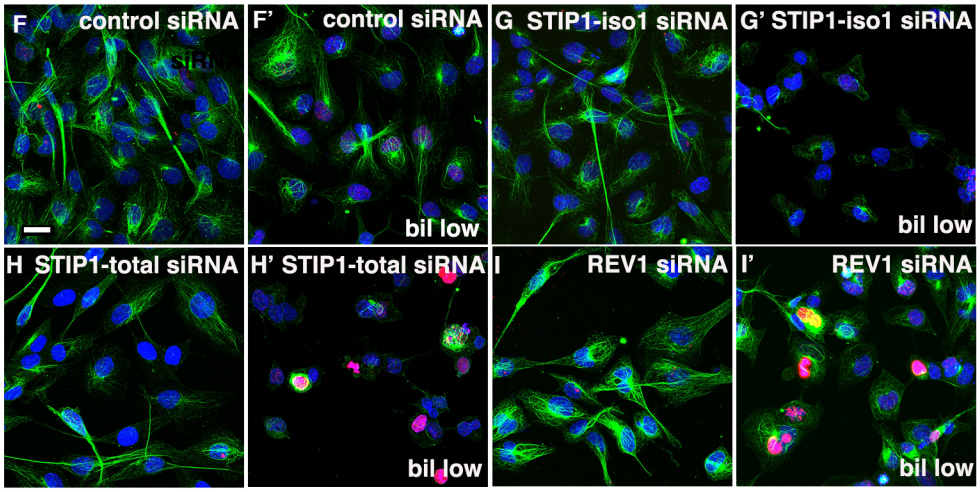
F control siRNA
F' control siRNA
bil low
G STIP1-iso1 siRNA
G' STIP1-iso1 siRNA
bil low
H STIP1-total siRNA
H' STIP1-total siRNA
bil low
I REV1 siRNA
I' REV1 siRNA
bil low

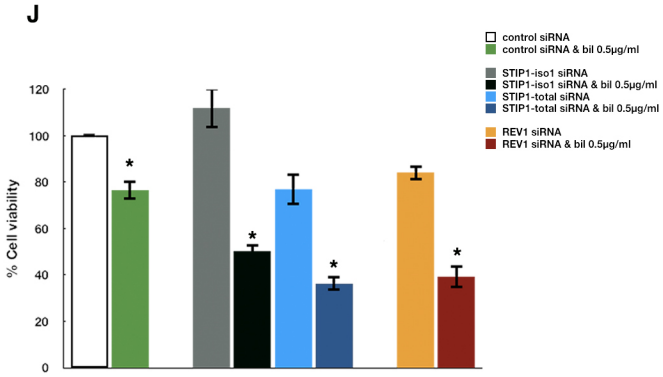
J
control siRNA
control siRNA & bil 0.5μg/ml
STIP1-iso1 siRNA
STIP1-iso1 siRNA & bil 0.5μg/ml
STIP1-total siRNA
STIP1-total siRNA & bil 0.5μg/ml
REV1 siRNA
REV1 siRNA & bil 0.5μg/ml
% Cell viability
120
100
80
60
40
20
0

Fig. 6

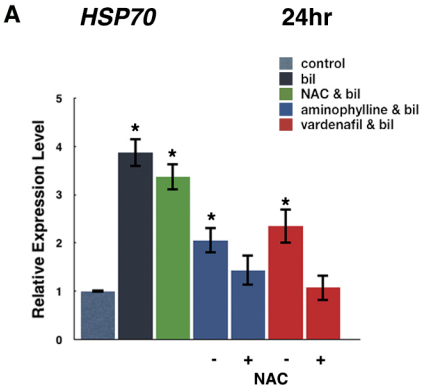
A
HSP70
24hr
control
bil
NAC & bil
aminophylline & bil
vardenafil & bil
Relative Expression Level
0
1
2
3
4
5
- + - +
NAC

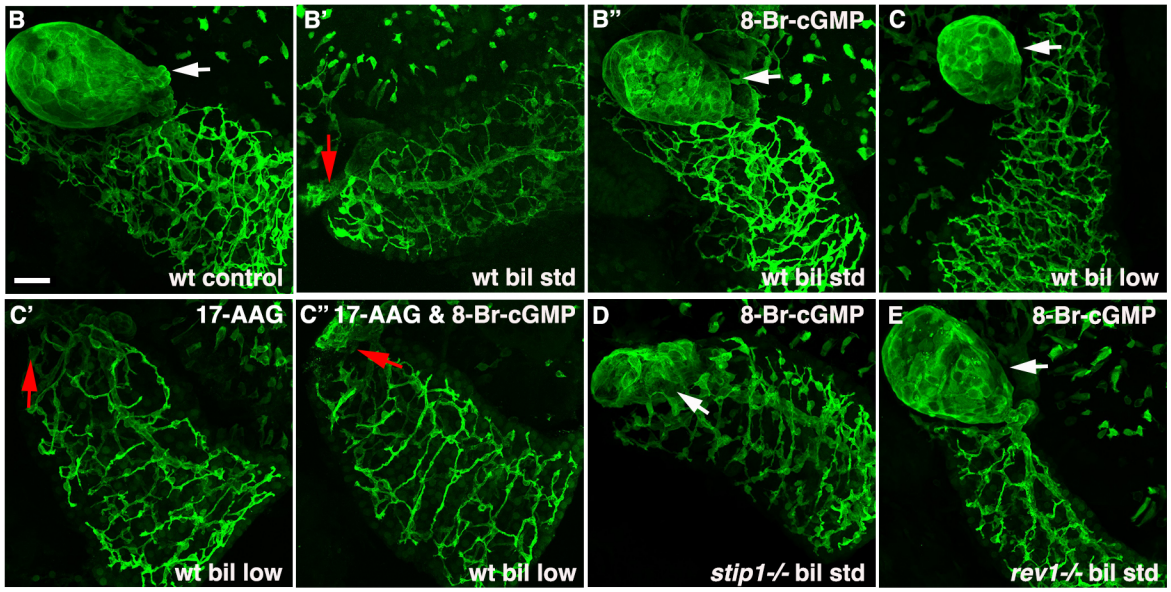
B
wt control
B'
wt bil std
B''
8-Br-cGMP
wt bil std
C
wt bil low
C'
17-AAG
wt bil low
C'' 17-AAG & 8-Br-cGMP
wt bil low
D
8-Br-cGMP
stip1-/- bil std
E
8-Br-cGMP
rev1-/- bil std

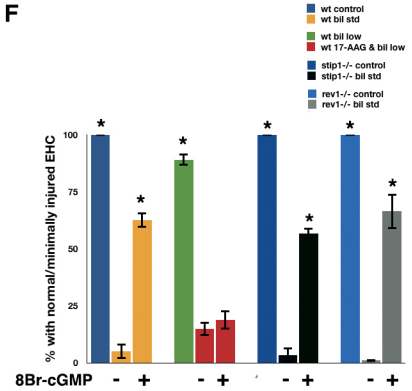
F
wt control
wt bil std
wt bil low
wt 17-AAG & bil low
stip1-/- control
stip1-/- bil std
rev1-/- control
rev1-/- bil std
% with normal/minimally injured EHC
0
25
50
75
100
8Br-cGMP
- + - + - + - +

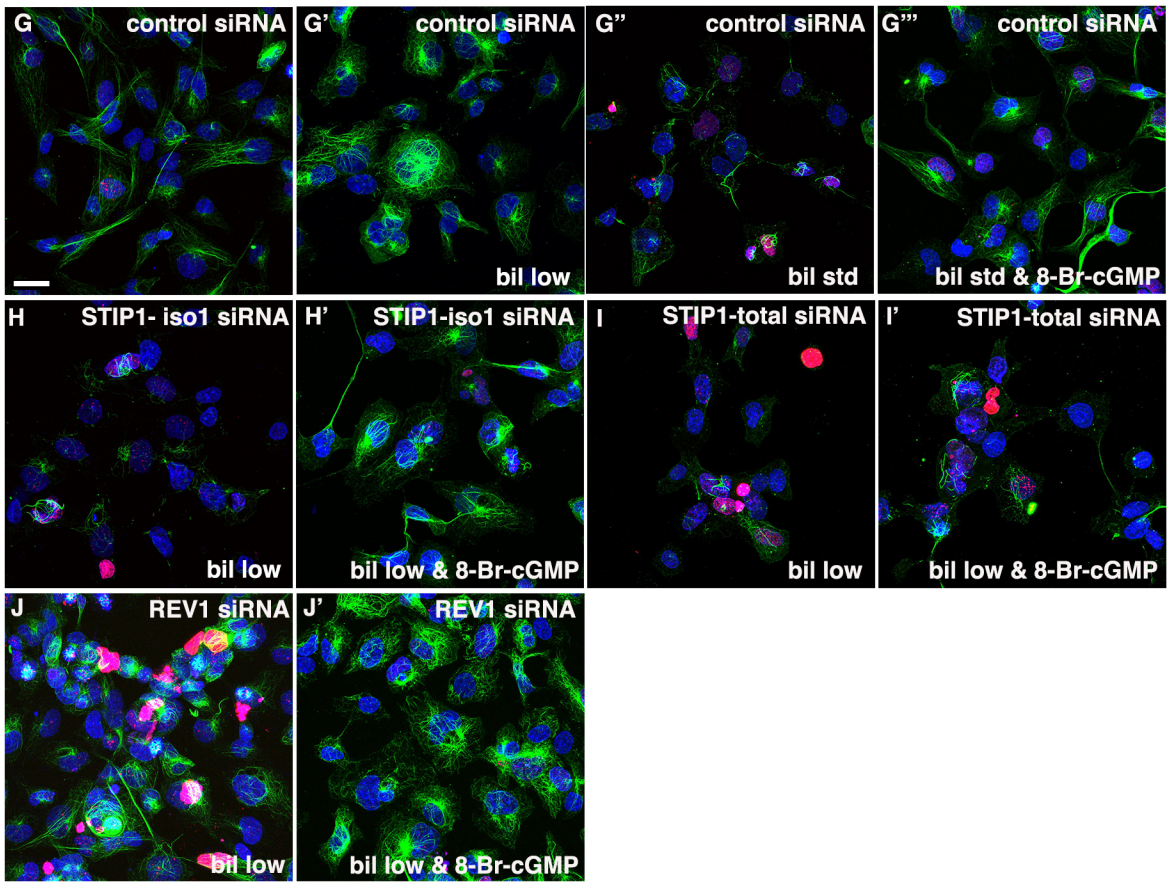
G
control siRNA
G'
control siRNA
bil low
G''
control siRNA
bil std
G'''
control siRNA
bil std & 8-Br-cGMP
H
STIP1- iso1 siRNA
bil low
H'
STIP1-iso1 siRNA
bil low & 8-Br-cGMP
I
STIP1-total siRNA
bil low
I'
STIP1-total siRNA
bil low & 8-Br-cGMP
J
REV1 siRNA
bil low
J'
REV1 siRNA
bil low & 8-Br-cGMP

Fig. 7

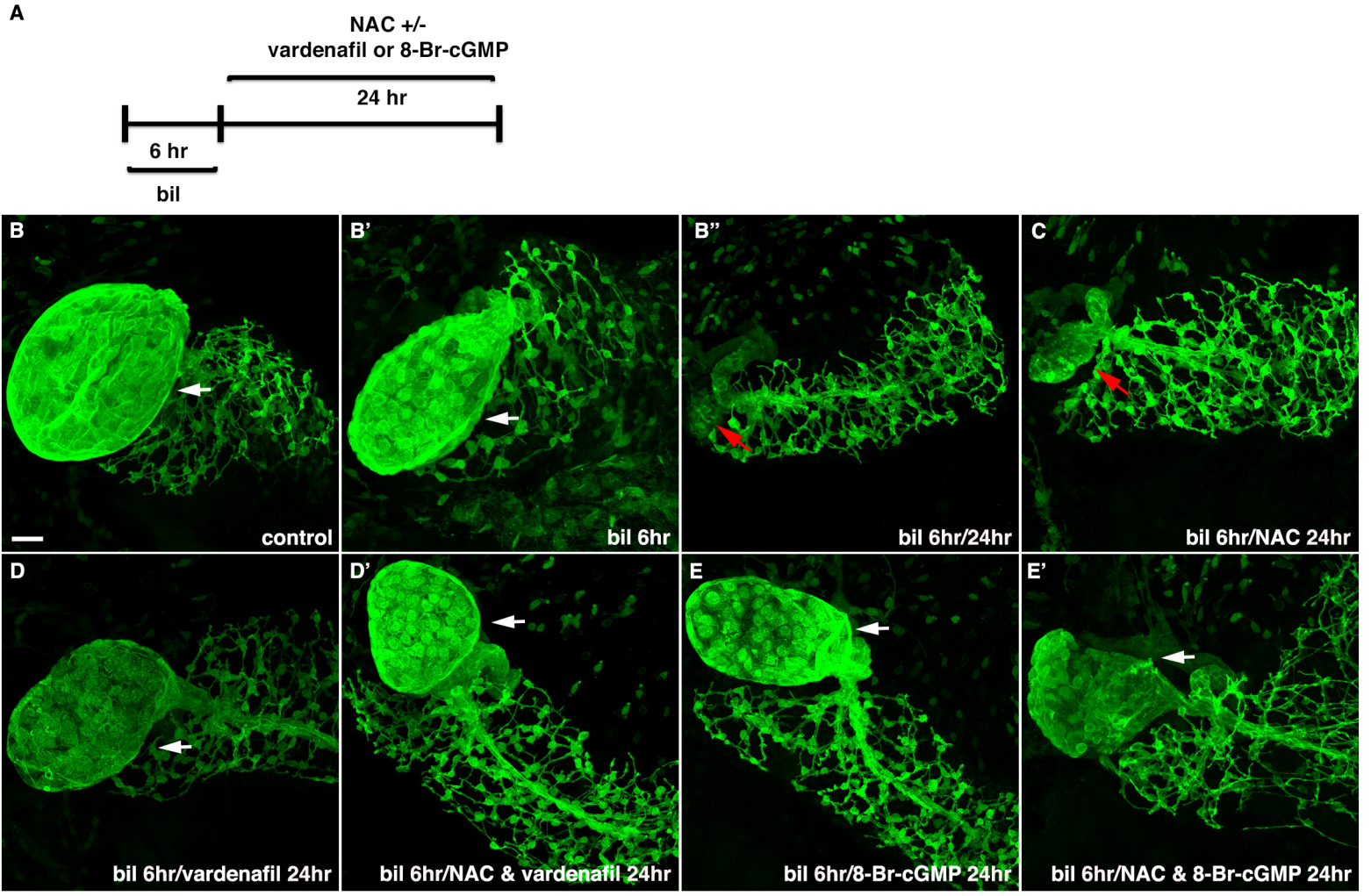
A
NAC +/-
vardenafil or 8-Br-cGMP
24 hr
6 hr
bil
B
control
B'
bil 6hr
B''
bil 6hr/24hr
C
bil 6hr/NAC 24hr
D
bil 6hr/vardenafil 24hr
D'
bil 6hr/NAC & vardenafil 24hr
E
bil 6hr/8-Br-cGMP 24hr
E'
bil 6hr/NAC & 8-Br-cGMP 24hr

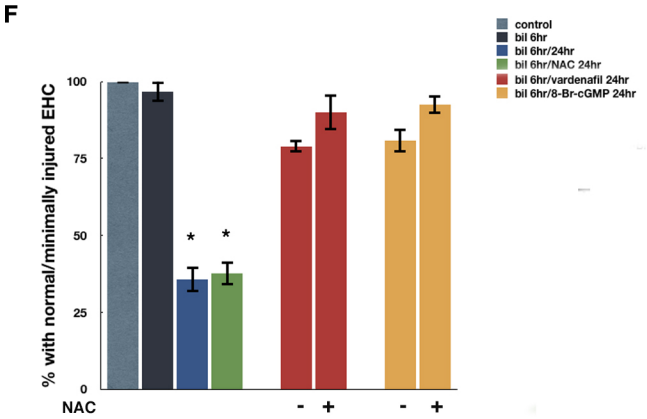
F
control
bil 6hr
bil 6hr/24hr
bil 6hr/NAC 24hr
bil 6hr/vardenafil 24hr
bil 6hr/8-Br-cGMP 24hr
% with normal/minimally injured EHC
100
75
50
25
0
*
*
NAC
-
+
-
+